Yttrium Iron Garnet (YIG) as Magnetic Nanoparticles for Enhanced Oil Recovery (EOR) using Electromagnetic Technique

By

Muhammad Faris Akram B. Azmi Rais

Dissertation submitted in partial fulfillment of

the requirement for the

Bachelor of Engineering (Hons)

(Petroleum Engineering)

SEPTEMBER 2013

Universiti Teknologi PETRONAS

Bandar Seri Iskandar

31750 Tronoh

Perak Darul Ridzuan

CERTIFICATION OF APPROVAL

Yttrium Iron Garnet (YIG) as Magnetic Nanoparticles for Enhanced Oil Recovery (EOR) using Electromagnetic Technique

By

Muhammad Faris Akram B. Azmi Rais

Dissertation submitted in partial fulfillment of

the requirement for the

Bachelor of Engineering (Hons)

(Petroleum Engineering)

Approved by,

_____

(DR HASSAN SOLEIMANI)

UNIVERSITI TEKNOLOGI PETRONAS

TRONOH, PERAK

September 2013

CERTIFICATION OF ORIGINALITY

This is to certify that I am responsible for the work submitted in this project, that the original work is my own except as specified in the references and acknowledgements, and that the original work contained herein have not been undertaken or done by unspecified sources or persons.

_____

MUHAMMAD FARIS AKRAM B. AZMI RAIS

ABSTRACT

Enhanced oil recovery (EOR) is currently the novel method to recover the remaining crude oil in the major oil field around the world. Enhanced oil recovery can be classified into 2 major component; chemical and thermal oil recoveries. The phenomenon of magnetic nanoparticles recently attracts the researcher because of the ability of nanoparticles to react with electromagnetic waves to disturb the oil in the reservoir. Despite the usage of many magnetic nanoparticles such as cobalt ferrite, another material like yttrium iron garnet is never been tested its performance. Yttrium iron garnet (YIG) is thermally stable in high temperature and it is the main reason why it is widely use in the microwave appliances. This is a good parameter for oil with high viscosities and instead of injecting hot water; the YIG will be injected as the nano fluid to recover the oil. Thus, this project is to investigate the potential of Yttrium iron garnet as magnetic nanoparticles for enhanced oil recovery using electromagnetic waves. The oil recovery of yttrium iron garnet (YIG) magnetic nanoparticles with Electromagnetic waves are 17.77% of the Original Oil in Place (OOIP) and the recovery of 43.64% of the remaining oil in the core.

ACKNOWLEDGEMENT

I would like to express my highest gratitude to UNIVERSITI TEKNOLOGI PETRONAS (UTP) for giving me the opportunity for me to complete the Final Year Dissertation. The gratitude also goes to my supervisor, Dr Hassan Soleimani and I would like to take this opportunity to thanks the supportive team from various departments for their excellent assistance throughout my final year project. I also would like to thank my co-supervisor, Professor Dr. Noorhana Binti Yahya in helping me throughout the project.

My appreciation also goes to Rasyada Abdul Latiff, Graduate Assistance. She has been very excellent and committed to teach and provide hands on training as a researcher in UTP. In addition, she is willing to share her valuable knowledge and experiences with me. I also would like to thank my supervisor for trusting and letting me conduct the experiment with her supervision; she also taught me about the Health, Safety, and Environment etiquette during my project period.

Lastly, I would like to express my special gratitude to my family for their endless support to me and MARA for sponsoring the scholarship to me.

TABLE OF CONTENTS

LIST OF FIGURES

LIST OF TABLES

CHAPTER 1

INTRODUCTION

1.1 Background Study

Nowadays, various Enhanced Oil Recovery (EOR) methods are applied to maximize the ultimate oil recovery and along the way have gained attention and interest in many oil & gas company. The recovery techniques always promise to be more efficient and cost effective, increase the recovery, environmentally friendly and most importantly the maximum profit obtain. A huge number of oil & gas operators were investing to this recovery method. It is imperative that the industry implement EOR projects now, in a fully integrated fashion. The operators were striving from research to incorporating operational readiness, and project execution with a greater sense of urgency.

The recoveries of oil were classified into three stages which are primary, secondary and tertiary recovery. Primary recovery is usually using natural reservoir energy such as gas drive, water drive or gravity drainage as shown as in Figure 1. All the natural reservoir energy displaces the oil from the reservoir into the wellbore and up to the surface. The primary recovery stage reaches its limit when the reservoir pressure is so low that the production rates will be uneconomical. The primary recovery can recover mostly 10% of the original oil in place (OOIP), but it depends on the field properties.

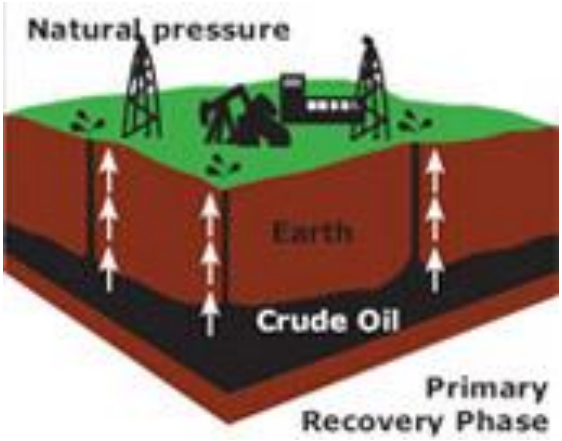

Figure 1 Primary recovery of oil (China Oilfield Technology Services Group Limited, 2007)

The secondary recovery is applied when the primary recovery is no longer profitable. External fluid such as water or gas is injected into the reservoir through injection wells located in the rock that has fluid communication with production wells. Further investment have to be made to build the injection well and facilities. The common secondary recovery technique is gas injection and waterflooding. The purpose of gas injection and waterflooding is supporting the reservoir pressure so that it can lift up the oil up to the surface as pictured in Figure 2. The secondary recovery is no longer a novel method when the injected fluid (water or gas) is produced in considerable amount from production wells. The primary and secondary recovery would contribute to recovery percentages up to 15% to 40% of original oil in place (OOIP).

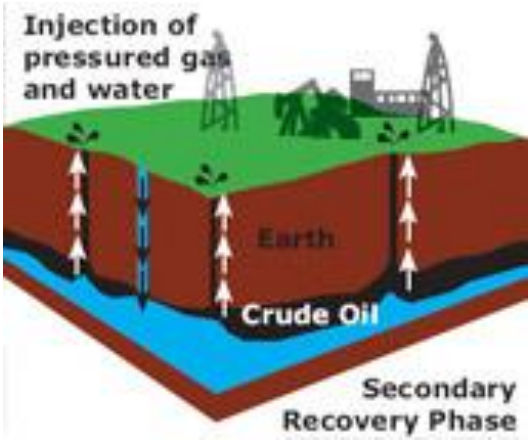

Figure 2 Secondary Recovery of Oil (China Oilfield Technology Services Group Limited, 2007)

Figure 3 shows tertiary recovery or well known as Enhanced Oil Recovery (EOR) are the latest stage in oil production. An EOR is enhancement method using sophisticated techniques that alter the OOIP. The main goal of EOR is to improve the sweep efficiency of oil. All of currently available EOR is based on one or more of two principles: increasing the capillary number and/or lowering the mobility ratio, compared to their waterflood values. Increasing the capillary number is reducing oil-water interfacial tension. The injectant mobility may be reduced by increasing water viscosity, reducing oil viscosity, reducing water permeability or all of the above. EOR processes are divided into four categories: thermal, gas, chemical, and other as shown in Table 1 (Lake & Walsh, 2008). The recovery of oil using EOR is expected to be approximately 20% to 30% of oil after primary and recovery process.

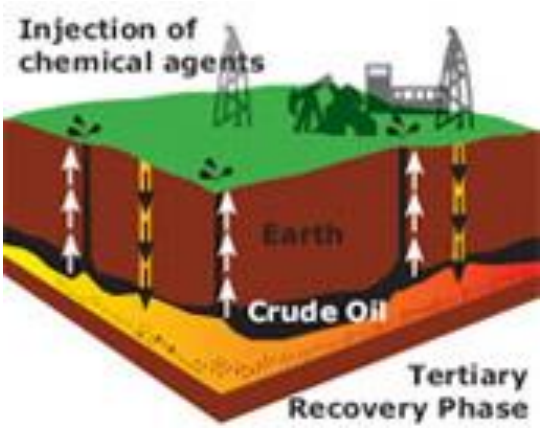

Figure 3 Tertiary recovery or enhanced oil recovery (EOR) (China Oilfield Technology Services Group Limited, 2007)

Table 1 EOR categories and processes

Thermal EOR processes	Gas EOR processes
• Steam flooding • Cyclic steam stimulation • In-situ combustion • Hot water flooding • Steam-assisted gravity drainage	• Oil miscible/immiscible • CO2 miscible • CO2 immiscible • Nitrogen • Flue gas (miscible and immiscible) • Gravity drainage
Chemical EOR processes	**Other EOR processes**
• Micellar-polymer • Polymer • Caustic/alkaline • Alkaline/surfactant	• Carbonated waterflood • Microbial • Electromagnetic heating

Thermal recovery comprises the techniques of steamflooding, cyclic steam simulation, and in situ combustion (United Energy Group, 2008). Figure 4 showing that steamflooding is a process of injecting high temperature steam into a reservoir to heat the oil. The result expected from steamflooding is to expand the oil and become less viscous; partially vaporizes, making the oil easier to move to the production wells. In addition, steamflooding is generally used in heavy oil reservoir.

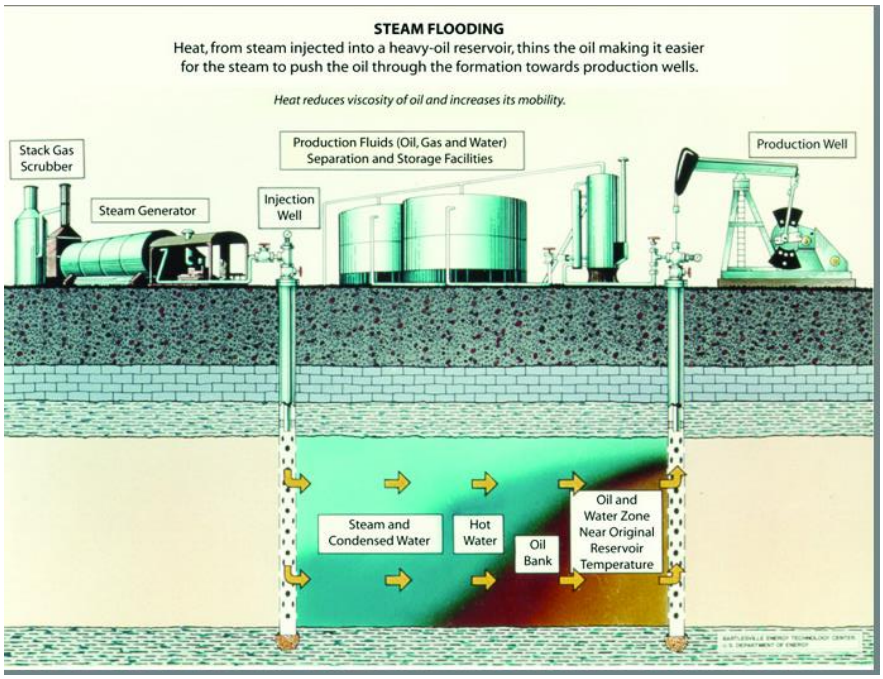

Figure 4 Enhanced Oil Recovery using steamflooding techniques (United Energy Group, 2008)

Cyclic steam simulation is also known as the "huff-and-puff" method. This method is applied to heavy oil reservoir to boost recovery during the primary production phase. The mechanism of cyclic steam simulation is the steam is injected into the reservoir, and then the well is shut in to allow the steam to heat the producing formation around the well. After ample time is given to the reservoir, the injection wells are placed back in production until the heat is dissipated with the production oil. The cycle may be repeated until the response becomes marginal because of declining natural reservoir pressure and increased water production (United Energy Group, 2008). At this stage a continuous steamflood is usually initiated to continue the heating and thinning of the oil and to support the declining reservoir pressure to increase the oil recovery as shown in Figure 5.

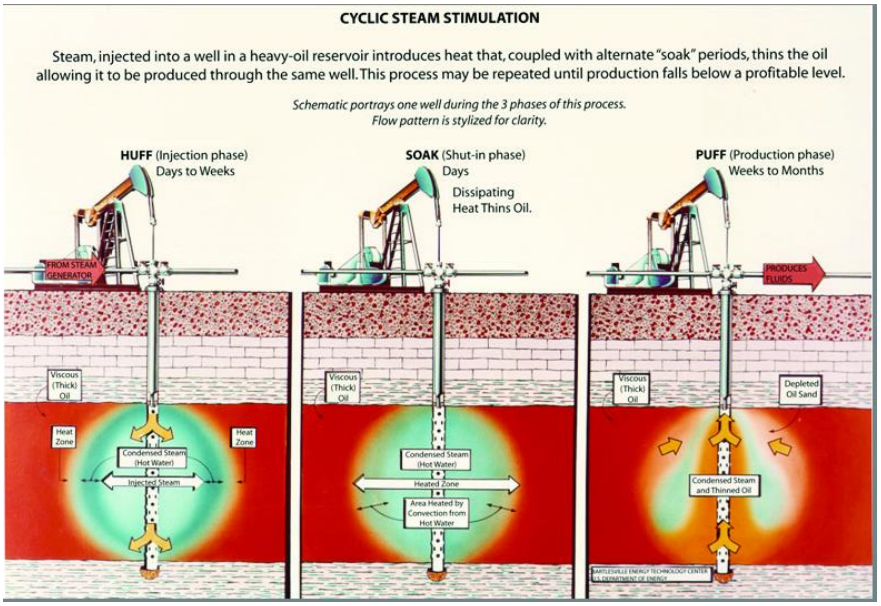

Figure 5 Enhanced Oil Recovery using cyclic steam combustion techniques (United Energy Group, 2008)

Lastly in thermal oil recovery technique is in situ combustion or "fireflooding". Heavy oil wells are targeted to be the mechanism to use in situ combustion because of the high viscosity of oil to be produced by conventional means. The in situ combustion is generally applied by igniting air to create a combustion zone that moves through formation towards the production wells. The intense heat forms zones of steam and vaporized oil that move in advanced of the combustion zone to production wells as shown in Figure 6.

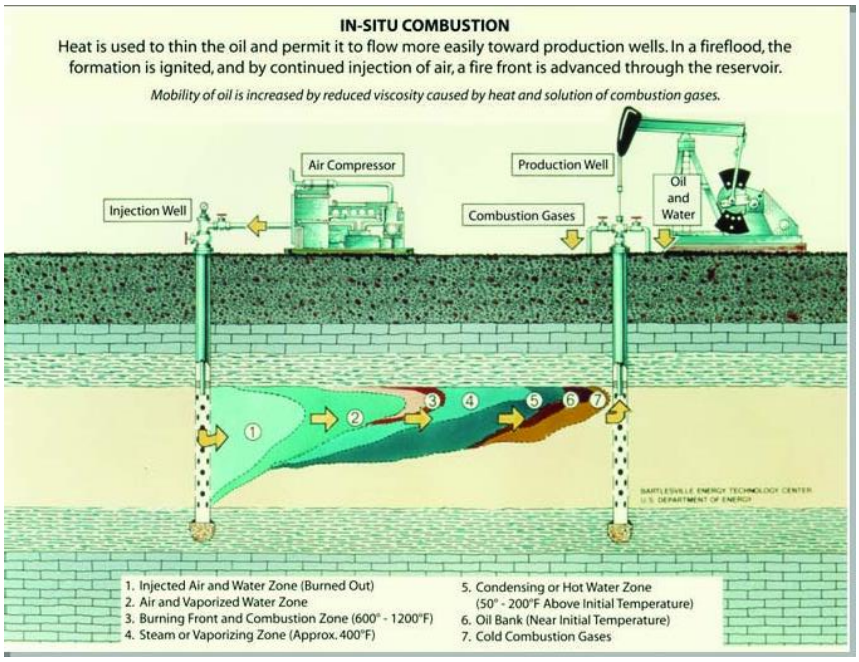

Figure 6 In situ combustion techniques for Enhanced Oil Recovery (EOR) (United Energy Group, 2008)

Other common enhanced oil recovery (EOR) techniques are chemical injection. One of the techniques is polymer flooding. Polymer is used under certain reservoir condition that lower the efficiency of a novel method of waterflooding, such as fractures or high-permeability regions that channel or redirect the flow of injected water, or heavy oil that resistant to move as shown in Figure 7. Water-soluble polymer is added to the waterflood allowing the water to move through more of the reservoir rock, resulting in a larger percentage of oil recovery.

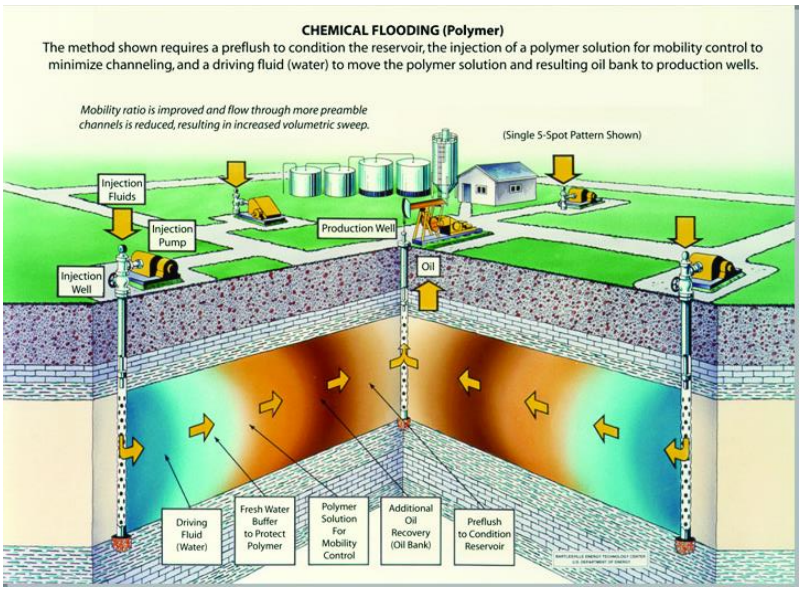

Figure 7 Polymer flooding process in EOR (United Energy Group, 2008)

In the recent studies researcher found that Electromagnetic (EM) waves have the potential to be one of the alternatives for enhanced oil recovery (EOR) technique. EM energy can be used as a source of thermal heating to reduce the viscosity of the oil in the reservoir which leads to the increase in production. Magnetic chemical is used as surfactant, alkali or polymer as the injectant in the reservoir. The main function of EM waves is to trigger the magnetic properties in the chemical. The magnetic chemical used in the studies is in nanoparticles, which is in very small size and able to pass through a narrow porous medium or low permeability zone. Further study of magnetic nanoparticles and its effect of EM waves for Enhanced Oil Recovery (EOR) are continued in this project using another material.

1.2 Problem Statement

Magnetic nanoparticles are a new material recently discovered as a potential material to be used in Enhanced Oil Recovery (EOR) using Electromagnetic (EM) technique. Figure 8 shows the chemical injection mechanism. The purpose of chemical injection is to increase the sweep efficiency in the reservoir by reducing the interfacial tension, increase the viscosity of displacing fluid (water) and decreasing the viscosity of displaced fluid (oil). Yttrium Iron Garnet (YIG) magnetic nanoparticles never been used in EOR, therefore the potential of YIG nanoparticles effect with EM is not yet been discovered.

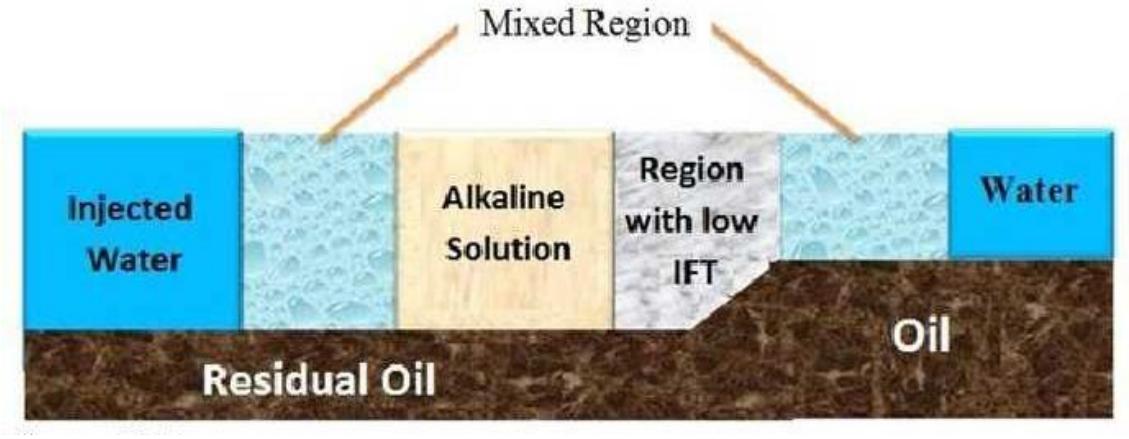

Figure 8 Chemical injection mechanisms

1.3 Objectives

The objectives of this project are to synthesize and characterize the Yttrium Iron Garnet (YIG) as the magnetic nanoparticles. Then, the nanoparticles were experimented through coreflooding tests to analyze the performance. Thus, to achieve the objectives of the project, the good nanoparticles of YIG need to be synthesized and tested that is able to meet the criteria.

1.4 Scope of Study

There are two part of work scope in this project. The first scope is to synthesize the material, which is Yttrium Iron Garnet (YIG) and characterize the magnetic nanoparticles. The second scope is the fluid-rock chemical evaluations which is coreflooding

1.5 Feasibility of Study

A time frame was planned accordingly to ensure the project is feasible within the timeline given. 2 semesters is given to the student to complete the project. Since, this project is involving 3 stages: synthesize and characterize of magnetic nanoparticles, and coreflooding test

CHAPTER 2

LITERATURE REVIEW

2.1 Nanoparticles

A nanoparticle is a small object that behaves as a whole unit in terms of its transport and properties (Mandal). In terms of diameter, fine particles cover a range between 100 and 2500 nanometers, while ultrafine particles are sized between 1 and 100 nanometers as shown in Figure 9. Nanoparticles may or may not exhibit size-related properties that are seen in fine particles. Despite being the size of the ultrafine particles individual molecules are usually not referred to as nanoparticles. Nanoclusters have at least one dimension between 1 and 10 nanometers and a narrow size distribution. Nano powders on the other hand are agglomerates of ultrafine particles, nanoparticles, or nanoclusters. Nano particle sized crystals are called nanocrystals.

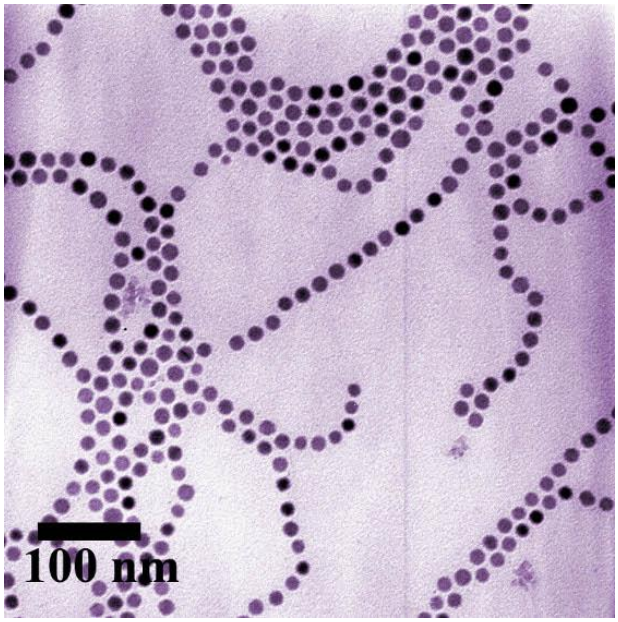

Figure 9 Colorized transmission electron micrograph showing chains of cobalt nanoparticles.

Nanoparticles are unique because of their large surface area and this dominates the contributions made by the small bulk of the material. Zinc oxide particles have been

found to have superior UV blocking properties compared to its bulk substitute. This is one of the reasons why it is often used in the preparation of sunscreen lotions.

Other examples of the physical properties of nanoparticles:

- Color – Nanoparticles of yellow gold and gray silicon are red in color
- Gold nanoparticles melt at much lower temperatures (~300 °C for 2.5 nm size) than the gold slabs (1064 °C)
- Absorption of solar radiation in photovoltaic cells is much higher in nanoparticles than it is in thin films of continuous sheets of bulk material - since the particles are smaller, they absorb greater amount of solar radiation.

Nanoparticles possess a variety of shapes and their names are characterized by their different shapes. For example, there are nanospheres that are spherical, nanoreefs, nanoboxes, nanoclusters, nanotubes etc. These shapes or morphologies sometimes arise spontaneously as an effect of a templating or directing agent during synthesis for example during miscellar emulsions or anodized alumina pores, or from the innate crystallographic growth patterns of the materials themselves (Mandal).

Controlling the morphology of nanoparticles is of key importance for exploiting their properties for their use in several emerging technologies. Optical filters and bio-sensors are among the many applications that use optical properties of gold nanoparticles and it requires anisotropy of the particle shape as larger shapes produce greater plasmon losses.

Despite the great importance of the morphology of nanoparticles, it is generally not well characterized and practically never controlled. However, this is of prime importance. For example, this is important in magnetic devices where well-defined magnetization axes and switching fields are required to store or to process information. The morphological characteristics to be taken into account are:

- Flatness
- Sphericity
- Aspect ratio

2.2 Magnetic Nanoparticles

A magnetic nanoparticle is a new remarkable phenomenon such as ferromagnetic, superparamagnetism, high field irreversibility, and high saturation field. The phenomena arise from finite size and surface effects that dominate the magnetic behavior of individual nanoparticles (Tartaj, Morales, Veintemillas-Verdaguer, Gonzalez-Carreno, et al., 2003). Magnetic nanoparticles is also attractive because it have a single magnetic domain particles and accordingly their magnetic properties and their mutual interaction can be studied without magnetic domain effect and quantum size effects can be studied because of their nanoparticle dimension. (Taketomi, Sorensen, & Klabunde, 2000).

Magnetic induction heating behavior in magnetic particles provides a benefit for biomedical applications, such as targeted drug delivery, diagnostics, and magnetic separation (Zhang & Zhai, 2011). The previous research conducted on heating of ferrite nano-materials. The magnetic induction heating of ferrite materials is originated from their power loss in alternating magnetic field. The total power loss (P_L) is composed of three parts, hysteresis loss (P_h), eddy current loss (P_e) and residual loss (P_r). Hysteresis loss is due to the irreversible magnetization process in alternating current (AC) magnetic field. Eddy current loss is the Joule loss due to eddy current induced by the alternating magnetic field and hence depends much on the electrical resistivity of the material. The physical origin of residual loss is more complicated. The residual loss cannot be separated straight forwardly from eddy current loss, nor even from hysteresis

loss easily. The irreversible process and the hysteresis loop changes with the amplitude and frequency of the AC field.

Yittrium Iron Garnet (YIG) is a ferromagnetic materials because their potential applications in microwave devices and magneto-optical information storage. YIG is also transparent to wavelengths exceeding 600 nm, which makes it a good candidate for atom-optical purposes, in particular, for realizing new kinds of atom traps. Transparency is needed since our idea to construct the trap is based on combining the repulsive potential caused by an evanescent electromagnetic field with the attractive potential formed by a static magnetic field. In this case, the magnetic field is produced by permanent-magnet structures patterned in the surface of a YIG film (Helsinki University of Technology, 2008). In this project the YIG is prepared using sol-gel method.

2.3 Electromagnetic wave

Maxwell equation stated that the magnetic field produced (B) is proportionally related to the current and the type of material used. The bigger current flow inside a conductor, and the higher the permeability of the material used, the bigger B field is produced (Islam, Wadadar, & Bansal, 1991). Magnetic field (B) and the electric field (E) is propagation perpendicularly with the same amplitude where the reduction in the field B intensity will cause the same amount of reduction in field E. Figure 10 show the field E and B propagating perpendicularly in a medium. The magnitude of Field E is proportional to the magnitude of field B.

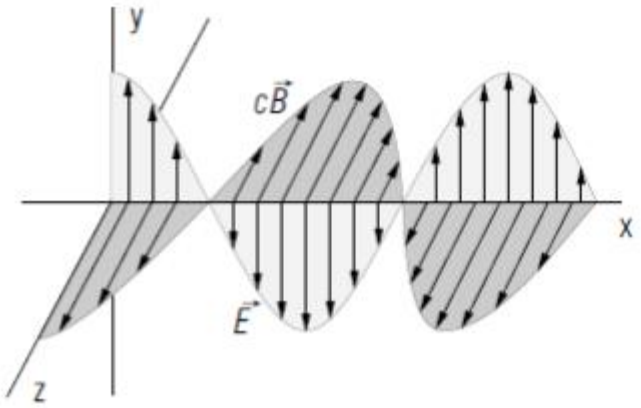

Figure 10 Electromagnetic (EM) waves propagation with respect to (x, y, z) direction.

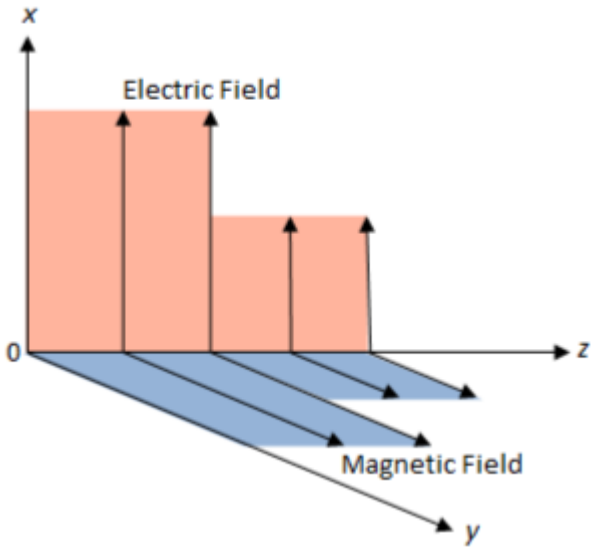

Figure 11 Magnetic Field (B) and Electric field (E) wave propagation.

Based on Maxwell equation (Islam, Wadadar, & Bansal, 1991).

$$B = \frac{\mu_0 I}{2\pi r}$$

where;

B = Magnetic field,

μ_0 = Magnetic Permeability

I = Current (A)

r= Distance

An electromagnetic (EM) wave is a self-propagating wave in a space of through matter. Light is not the only example of an electromagnetic wave. Other electromagnetic waves include the microwaves, and the radio waves. An electromagnetic wave can be created by accelerating charges; moving charges back and forth will produce oscillating electric and magnetic fields. A constant current produces a constant magnetic field, while a changing current produces a changing field. A steadily-changing magnetic field can induce a constant voltage, while an oscillating magnetic field can induce an oscillating voltage.

There are two key to understanding electromagnetic waves which are an oscillating electric field generates an oscillating magnetic field and an oscillating magnetic field generates an oscillating electric field. An electromagnetic wave (such as a radio wave) propagates outwards from the source (an antenna, perhaps) at the speed of light. What this means in practice is that the source has created oscillating electric and magnetic fields, perpendicular to each other, that travel away from the source. The E and B fields, along with being perpendicular to each other, are perpendicular to the direction the wave travels, meaning that an electromagnetic wave is a transverse wave. The energy of the wave is stored in the electric and magnetic fields.

An electromagnetic wave, although it carries no mass, does carry energy. It also has momentum, and can exert pressure (known as radiation pressure). The energy carried by an electromagnetic wave is proportional to the frequency of the wave. The wavelength

and frequency of the wave are connected via the speed of light. Electromagnetic waves are split into different categories based on their frequency (or, equivalently, on their wavelength). In other words, we split up the electromagnetic spectrum based on frequency. Visible light, for example, ranges from violet to red. Violet light has a wavelength of 400 nm, and a frequency of 7.5×10^{14} Hz. Red light has a wavelength of 700 nm, and a frequency of 4.3×10^{14} Hz. Any electromagnetic wave with a frequency (or wavelength) between those extremes can be seen by humans.

Visible light makes up a very small part of the full electromagnetic spectrum. Electromagnetic waves that are of higher energy than visible light (higher frequency, shorter wavelength) include ultraviolet light, X-rays, and gamma rays. Lower energy waves (lower frequency, longer wavelength) include infrared light, microwaves, and radio and television waves.

2.4 Electromagnetic (EM) transmitter

Electromagnetic (EM) consists of several system. One of the systems is time-domain electromagnetic system (TEM) which measures the EM as a function of time. Meanwhile the frequency-domain electromagnetic system (FEM) measures the EM waves with respect to one or more frequencies. EM systems are also containing passive and active. The passive system is using the natural ground sound signal (i.e. magnetotellurics). The main sources of passive EM system are lightning, magnetosphere activities. On the other hand, for active EM system is using transmitter to induce ground current. The current usages of EM system in oil & gas development are to detect the ground water contamination, salt water intrusion, and mapping geology soil.

Shape and size of a transmitter determine the effectiveness on how much the energy extracted from the EM waves. Therefore, an antenna is designed so that it can radiate and receive EM energy with directional and polarization properties suitable for the scope of work. Antenna commonly consists of two components that are used to radiate electric field (i.e. dipole antenna). The two conductors in antenna components act like a plate of capacitor with the field between them projecting out into space rather than

being confined between plates. The other magnetic field antennas are made of coils which act as a conductor. The inductor fields are projected out into space rather than being confined to a closed magnetic circuit. The properties of antenna are governed by its shape, size and material. The resistivity and conductivity of an antenna are:

$$R = \frac{\rho l}{A} \text{ and } \rho = \frac{1}{\alpha}$$

Where; R = Resistance

ρ = Resistivity

α = Conductivity

l = Length

A = Area

CHAPTER 3

METHODOLOGY

3.1 Project flowchart

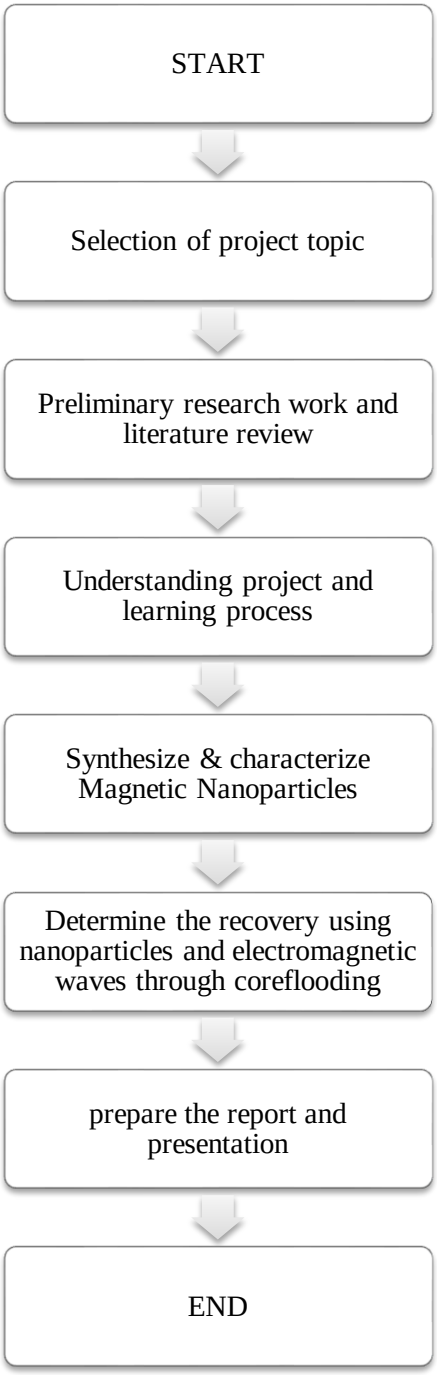

3.2 Synthesizing process

The preparation of Yttrium iron garnet (YIG) is using stoichiometric mixtures of nitrates iron (III) and Yttrium (III) as shown in Figure 12. The mixtures of both chemical were dissolved in an aqueous solution of acid and the resulting solution was heated at 80^{o}C to obtain the gel (Vaqueiro, Crosnier-Lopez, & Lopez Quintela, 1996).

Figure 12 Y(NO_3) and Fe(NO_3) chemical reagents

To obtain the YIG samples, gels were dried at 110^{o}C for 36 hours and going through heat treatment process for 2 and 12 hours.

3.3 Characterization: X-Ray Diffraction analysis

The samples are characterized using X-Ray Diffraction (XRD) method as shown in Figure 13. Based on the figure below the temperature of 800°C and 900°C for heat treatment is the optimal value to obtain Yttrium iron garnet (YIG).

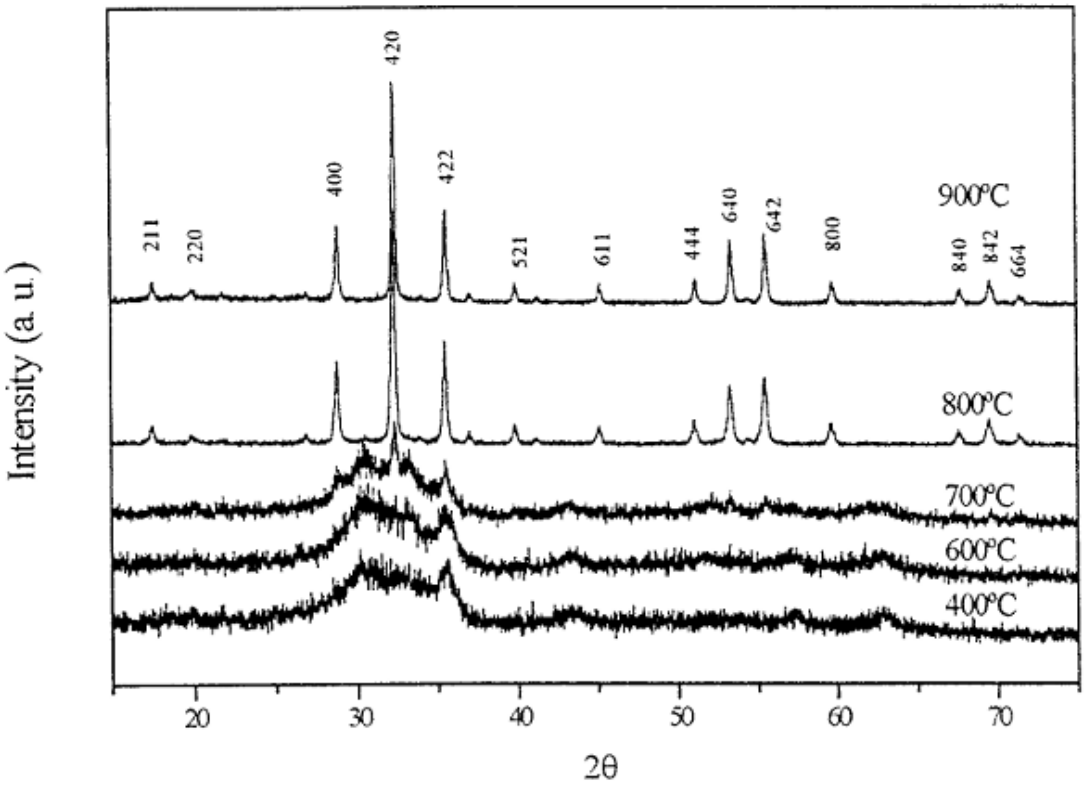

Figure 13 XRD result for YIG characterization (Vaqueiro, Crosnier-Lopez, & Lopez Quintela, 1996)

Meanwhile, heat treatment period is also affecting the crystallite size of the nanoparticles. Figure 14 shows the mean size of YIG crystal at 800°C with various heating time. Therefore, 2 hours of heat treatment is chosen to be done in this project to get the smallest mean size of YIG nanoparticles.

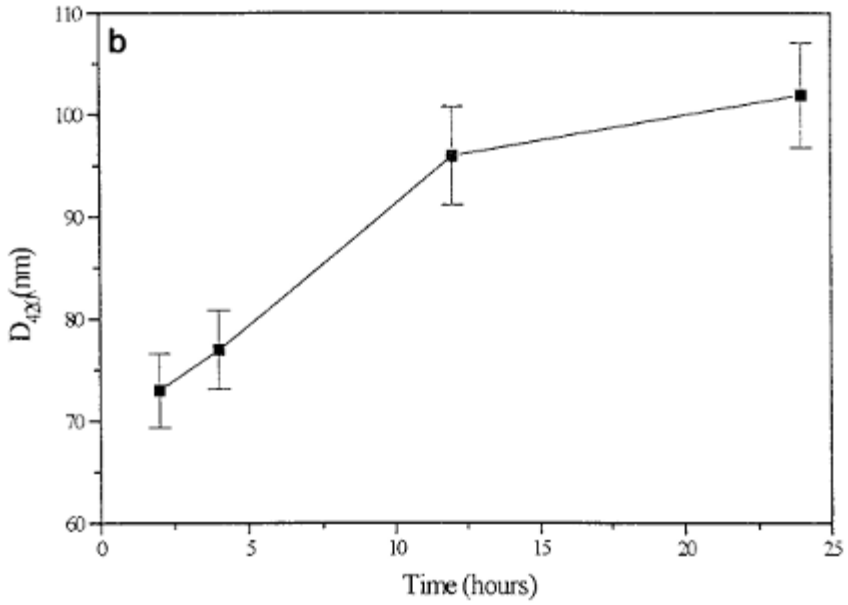

Figure 14 YIG samples at 800°C with different heating time

3.4 Characterization: Transmission Electron Microscopy (TEM) analysis

The Yttrium iron garnet is further tested with Transmission electron microscopy (TEM) to obtain the mean particles size. The thin specimens for TEM were obtained by ultrasonically dispersing the particles in n-butanol and disposing drops of this suspension on a copper grid covered with a holey carbon (Vaqueiro, Crosnier-Lopez, & Lopez Quintela, 1996). The test was performed with a JEOL-2010 electron microscope operating at 200kV and equipped with a side entry ±30° double tilt specimen holder. The analysis was done using KEVEX energy-dispersive X-ray spectrometer coupled with the Tem to allow approximation of the composition of the small particles. TEM was used to study the composition, shape, size, size distribution and crystallinity of particles. Figure 15 shows the morphology and size distribution fot YIG particles at 800°C with the mean size of 40nm.

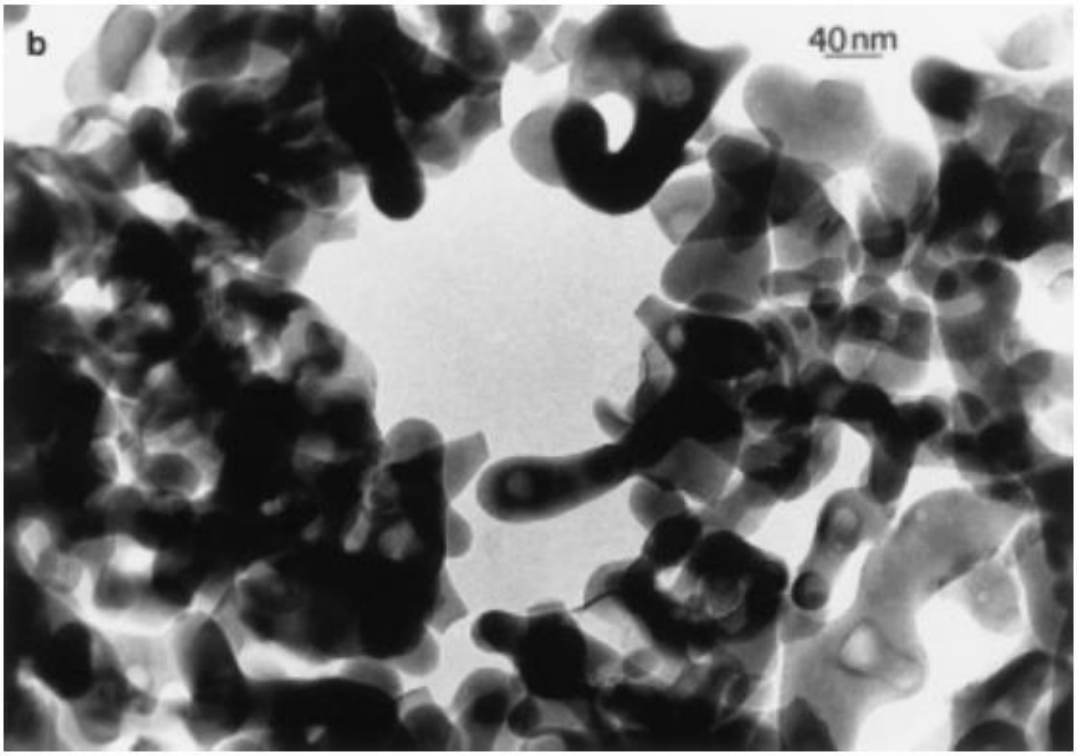

Figure 15 TEM results for 800°C YIG particles

3.5 Characterization: Vibrating sample magnetometer (VSM) Analysis

This analysis is to determine the magnetic properties of the particles. The analysis procedure begins with placing the sample inside a uniform magnetic field to magnetize the sample. Then, the sample is tested with sinusoidal vibration. By measuring the field of an external electromagnet, it is possible to analyze the hysteresis loop of the particles.

3.6 Coreflooding

The coreflooding test is to determine the recovery factor of the nanoparticles with electromagnetic waves. The coreflooding setup is shown in Figure 16.

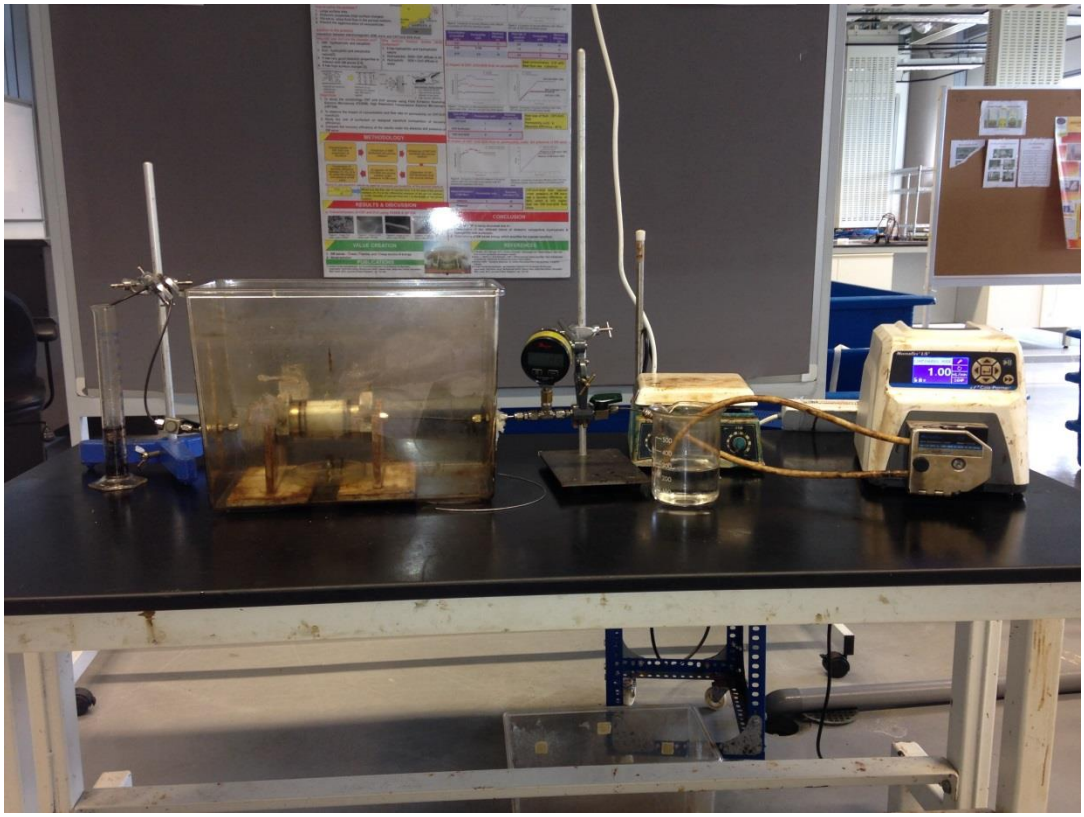

Figure 16 Coreflooding setup

The setup consist of pump, pressure gauge, core flooding tank, effluent collector, core holder and injection inlet. The pump is automatic with a default setting of continuous mode of injection of 1 mL/min flowrate. The pressure gauge is used to determine the pressure reading of the liquid injected into the core. The core holder is specifically design to ensure the magnetic nanoparticles is not attracted to the core holder, therefore, a PVC plastics is used. The pump used in the coreflooding test to govern the flowrate of oil, water, and nanoparticles injection is shown in Figure 17. The pressure gauge used is shown in Figure 18.

Figure 17 Masterflex US pump

Figure 18 Pressure Gauge to determine the pressure injection

Figure 19 shows core is setup with filling the PVC pipe with a glass beads until its fill all the space inside the plastic PVC, then 2 core holders is used to seal the glass beads. The core is sealed tightly to prevent any leaking from the core. Then, the core is weighted to obtain the dry weight.

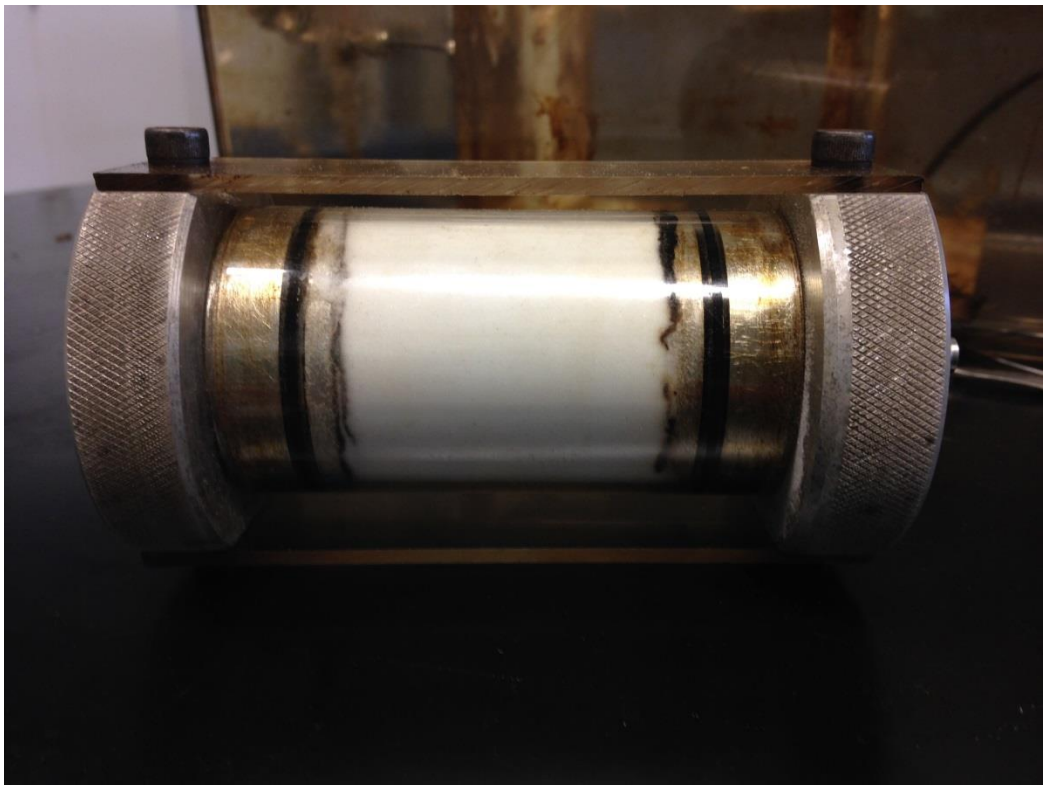

Figure 19 Core setup with a glass beads

The core holder is placed in the coreflooding setup and brine is injected to saturate the core. The injection takes place for 1 hour and the brine is allowed to settle down for another one hour. The volume of brine in the effluent collector is recorded. Then, the weight of the core with brine is weighted to determine pore volume. The calculation of pore volume is using following equation:

$$Pore\ Volume = \frac{(wet\ weight - dry\ weight)}{Density\ of\ brine}$$

After saturated the core for over 1 hour the crude oil is injected into the core. The volume of oil in the core is measured by the volume of brine that was displaced from the core. The oil in the core is allowed to settle down for over an hour before the waterflooding test is done. The core saturated by oil is shown in Figure 20.

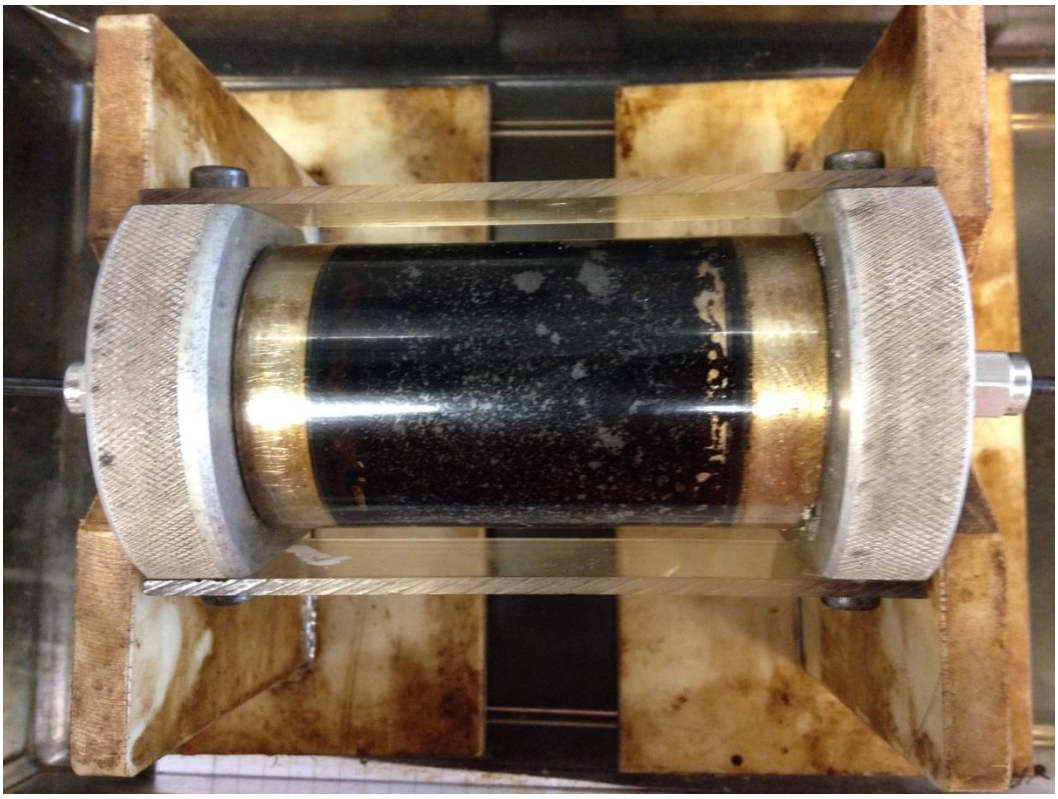

Figure 20 Core that is saturated by oil

The waterflooding is done to completed the secondary recovery mechanism before proceeding with nanoparticles injection for the enhanced oil recovery. The recovery factor for water injection is usually varies from 35-50% and the recovery factor for EOR is ranging from 10-15% of the remaining oil. The nanoparticle is prepared at a specific concentration and sonicated using ultra sonic equipment for 20 minutes. The nanoparticles is injected at a constant flowrate of 1 mL/min.

3.7 Gantt chart

FYP	Week	1	2	3	4	5	6	7	8	9	10	11	12	13	14	15	16	17	18	19	20	21	22	23	24	25	26	27	28
Progress	Month	June				July				August				September				October				November				December			
Topic selection																													
Research work & Proposal																													
Submission of Proposal																													
Proposal Defence																													
Synthesize - Yttrium Iron Garnet																													
Submission of Interim Report																													
Characterization of Yttrium iron garnet																													
Experimentation – Core flooding																													
Optimization of nanoparticles																													
Submission of Progress report																													
Submission of Final draft of report & Technical paper																													
Viva																													

3.8 Tools required

3.4.1 X-Ray diffraction (XRD)

X-ray scattering techniques are a non-destructive analytical method to determine the crystallite size, chemical composition and physical properties of the material. This technique is based on observing the scattered intensity of an X-ray beam hitting a material as a function of incident and scattered angle, polarization and wavelength or energy. X-ray diffraction also find the geometry or shape of a molecule using X-rays.

3.4.2 Transmission Electron Microscope (TEM)

A transmission electron microscope (TEM) is an analytical tool allowing visualization and analysis of specimens in the realms of microspace (1 micron/1μm = 10^{-6}m) to nanospace (1 nanometer/nm = 10^{-9}m). The TEM reveals levels of detail and complexity inaccessible by light microscopy because it uses a focused beam of high energy electrons. It allows detailed micro-structural examination through high-resolution and high magnification imaging. TEM is used to study the composition, shape, size, size distribution and crystallinity of particles through diffraction pattern, X-ray and electron-energy analysis.

CHAPTER 4

RESULT

4.1 Yttrium Iron Garnet (YIG) synthesizing & characterization process by using nitric acid as a solvent

The magnetic nanoparticles of Yttrium iron garnet (YIG) is prepared using sol-gel combustion method. The mixture of iron (III) nitrates, $Fe(NO_3)_3$ and yttrium (III) nitrates $Y(NO_3)_3$ are mixed together in an aqueous solution of Nitric acid, $C_6H_8O_7$. The molar number of iron (III) nitrates is 0.01mol and yttrium (III) nitrate is 0.006mol. The aqueous solution of citric acid is in 0.05mol. The ratio of three component iron (III) nitrate, yttrium (III) nitrate, and citric acid is 3:5:16. The ratio of mixture of chemical with acid is 1:1.

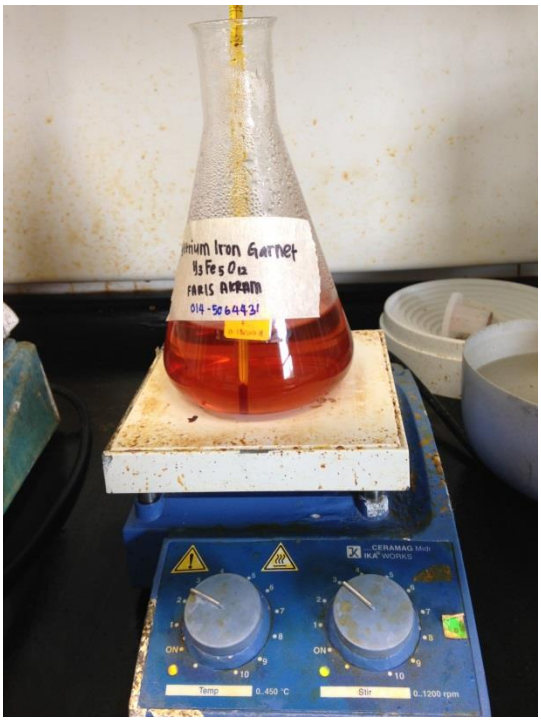

Figure 21 the mixture of yttrium, iron nitrate with nitric acid.

Figure 21 is showing the solution were mixed with water and heated at 80^{o}C for several hours until the gel is formed. After the gel form is obtained, the mixture is dried initially at 110^{o}C for 36 hour as pictured in Figure 22.

Figure 22 Yttrium Iron Garnet (YIG) after drying for 36 hours.

The main purpose of drying the gel formation is to eliminate the water content. The YIG sample is finished when the sample that already dried is undergo the annealing process with the temperature of 800^{o}C as shown in Figure 23. Based on literature by P. Vaqueiro, et al., 1996 it is said that the higher the temperature of annealing, the smaller the particle size. The particles size obtains are ranging from 20 to 500 nanometers and particles exhibit a rounded surface morphology.

Figure 23 Yttrium Iron Garnet after annealing at 800^{o}C for 2 hour

The yttrium iron garnet powder is obtained after undergoes heat treatment of 800^{o}C for 2 hours. The sample is taken to X-Ray diffraction (XRD) to determine the crystallite size. Figure 24 shows the result of XRD. Based on the figure below the red legend shows the most identical chemical composition to the sample synthesized which yttrium iron oxide. Therefore, an approach of re-anneal the sample at higher temperature is done to see whether the YIG is successfully synthesizes. The result of XRD of YIG at re-annealed temperature of 1000^{o}C is shown in Figure 25. Based on the analysis, the YIG is detected in the XRD, but the sample also contains a huge trace of hematite (Fe_2O_3). Therefore, it is concluded that the synthesizing process needed to be improvised to minimized the hematite trace in the YIG sample.

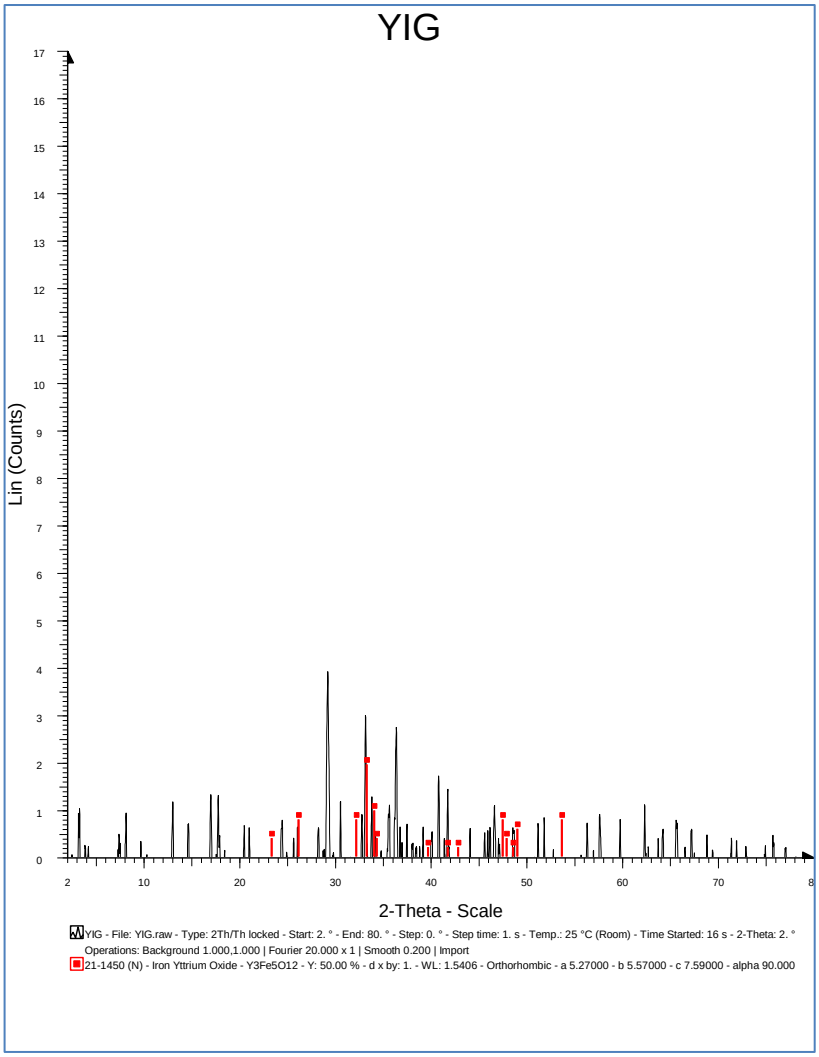

Figure 24 Result obtained from XRD and comparison between reference materials

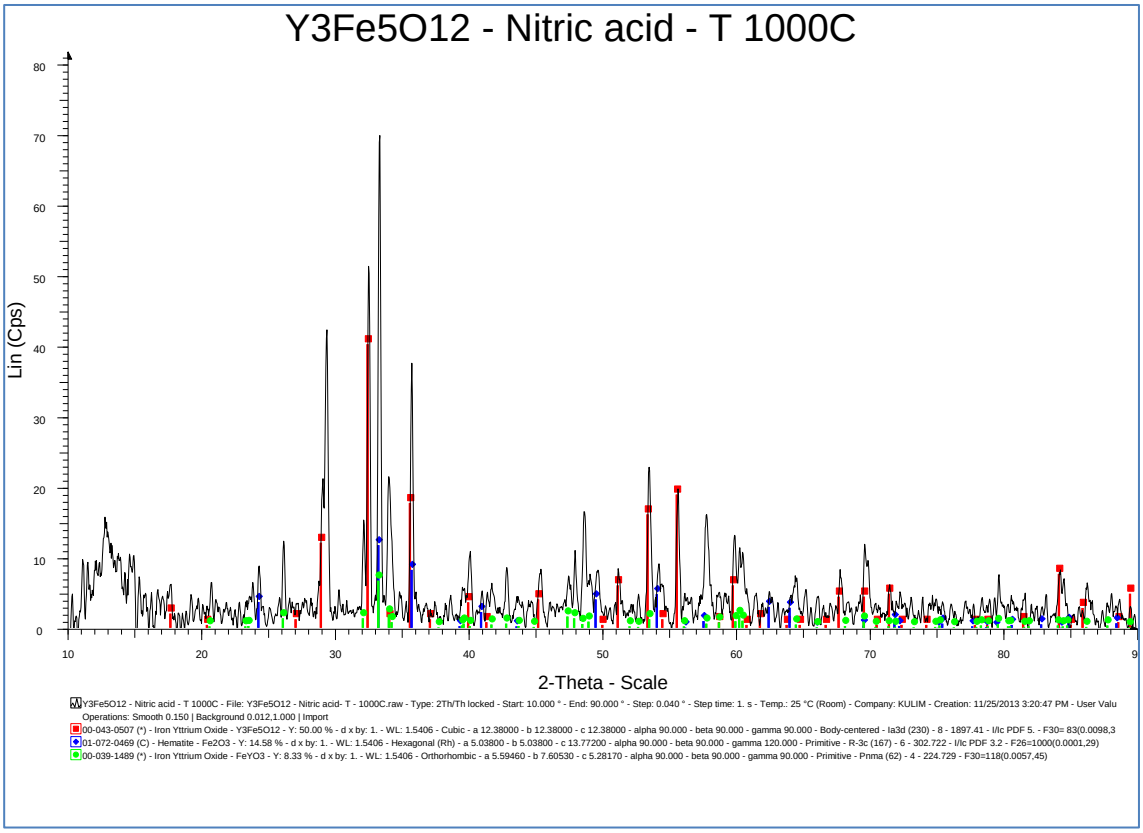

Figure 25 XRD result of YIG sample at re-annealed temperature of 1000^{o}C

4.2 Yttrium Iron Garnet (YIG) synthesizing & characterization process by using citric acid as a solvent

Another batch of yttrium iron garnet are synthesized using the same sol-gel method but with the different solvent which is Citric Acid ($C_6H_8O_7$). The same ratio of 3:5 is used in the process. The calculation of chemical reagent is illustrated below:

$$Y(NO_3) + Fe(NO_3) \rightarrow Y_3Fe_5O_{12}$$

Mass of $Y(NO_3)$ = no. of mol x molecular weight

= 0.006 mol x 383.01g/mol

= 2.298 g

Mass of $Fe(NO_3)$ = no. of mol x molecular weight

= 0.01 mol x 404.00/mol

= 4.04 g

Mass of ($C_6H_8O_7$) = no. of mol x molecular weight

= 0. 1 mol x 192.124 g/mol

= 19.22 g

Since the ratio of $Y(NO_3)$:$Fe(NO_3)$ is 3:5, the total mass for both chemical is 6.894g of $Y(NO_3)$ and 20.2g of $Fe(NO_3)$. A ratio of 1:1 is used to determine the solvent mass. The chemical reagent is diluted into 50mL of distilled water using auto-stirrer. Then, the acid is added into the beaker until the chemical mix vigorously. The samples are stirred heated at 80^{o}C. The sol-gel is obtained after 2 hours and the sample is dried at 110^{o}C for 36 hours as shown in Figure 26.

Figure 26 Yttrium Iron Garnet (YIG) sample after drying process

The samples are crushed and undergo heat treatment at 3 different temperatures for 2 hours. According to the literature, the best temperature to obtain smallest particles size is 800^{o}C to 1300^{o}C. Figure 27 shows the particles for YIG after heat treatment process.

Figure 27 Three samples after 3 differences heat treatment temperature

All the samples were sent for X-Ray Diffraction (XRD) test. The XRD result of YIG sample at temperature of 800^{o}C is shown in Figure 27. The sample is successfully characterized, but it is observed that the XRD wavelength consist a lot of noise and huge trace of hematite in the sample. Therefore, it is assumed that the sample is inadmissible. Figure 28 is the XRD result analysis of 1000^{o}C of yttrium iron garnet using citric acid as a solvent also does not gives an admissible result. Therefore, an approach of re-annealing the entire sample with the higher temperature is taken to minimize the trace of hematite in the sample and to obtain a clearer XRD wavelength.

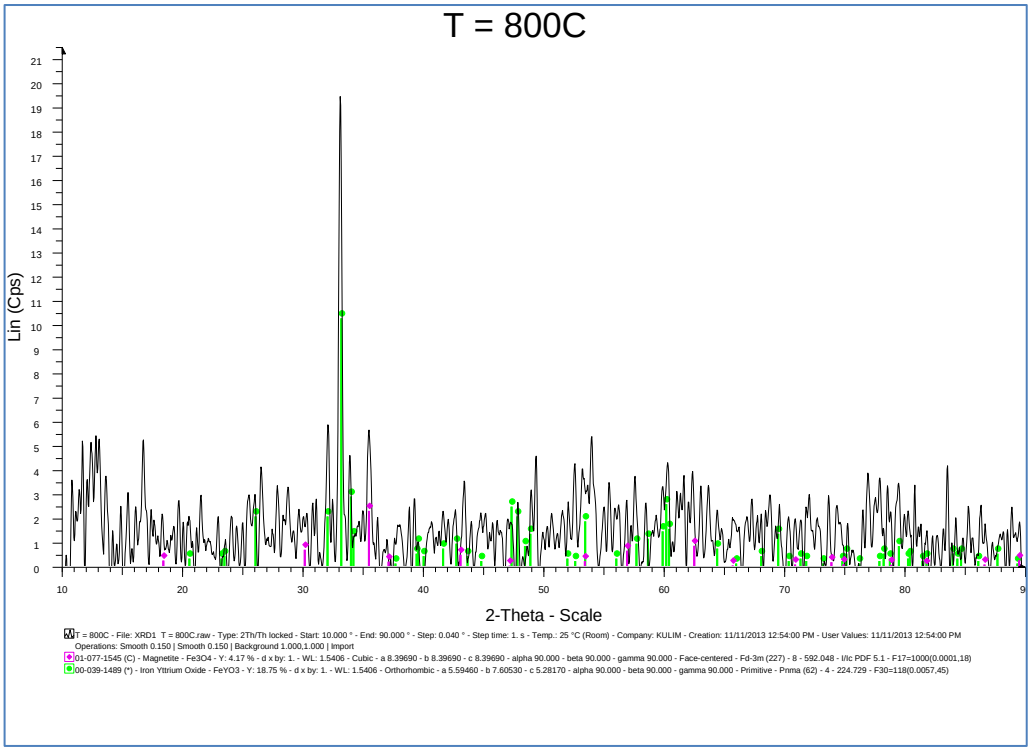

Figure 28 XRD result of 800°C of YIG

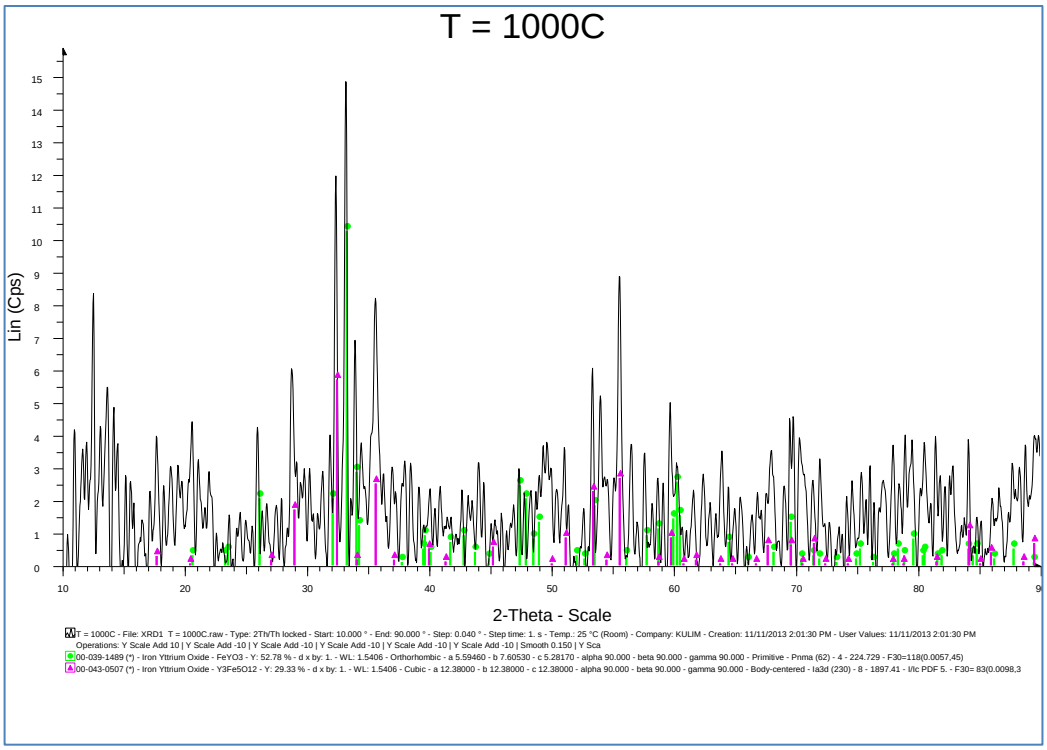

Figure 29 XRD result of 1000°C of YIG

All the samples are going through a second heat treatment with an additional 200^{o}C. The YIG at 800^{o}C is re-annealed at temperature of 1000oC and the sample of 1000^{o}C is re-annealed at 1200^{o}C. The XRD result of 1000^{o}C YIG is shown in Figure 30. Based on the result, the YIG particle is obtained with a small trace of hematite. The results of XRD of 1200^{o}C YIG is shown in Figure 31.

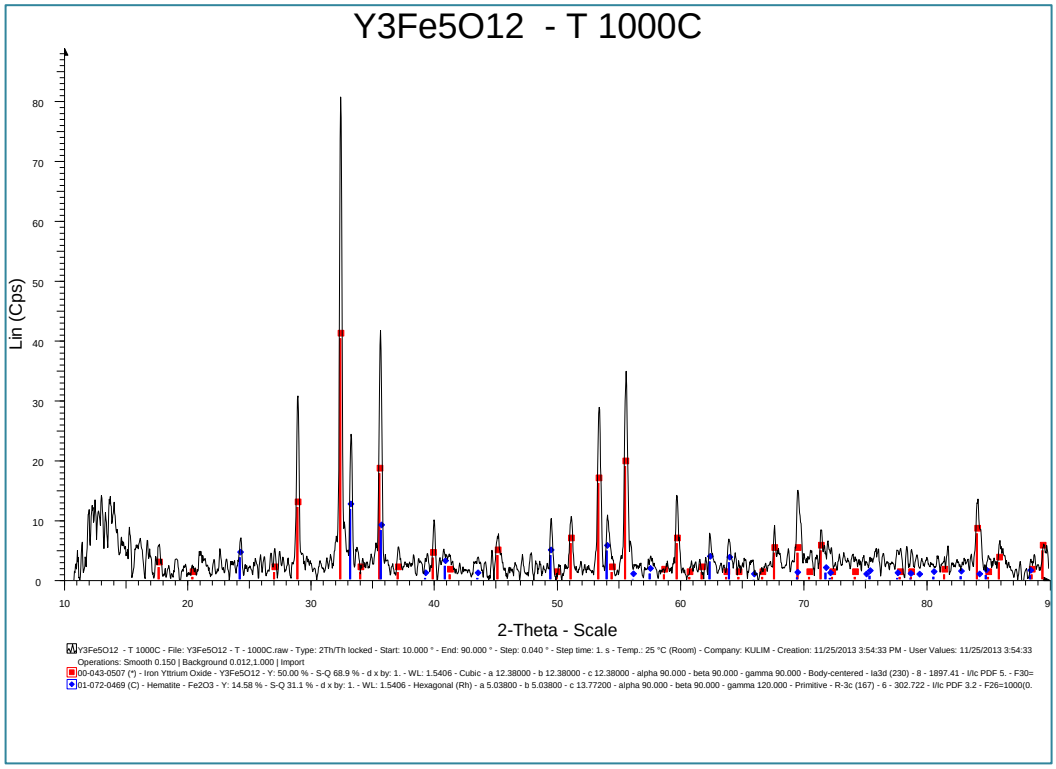

Figure 30 The XRD result of 800^{o}C of YIG that is re-annealed at 1000^{o}C

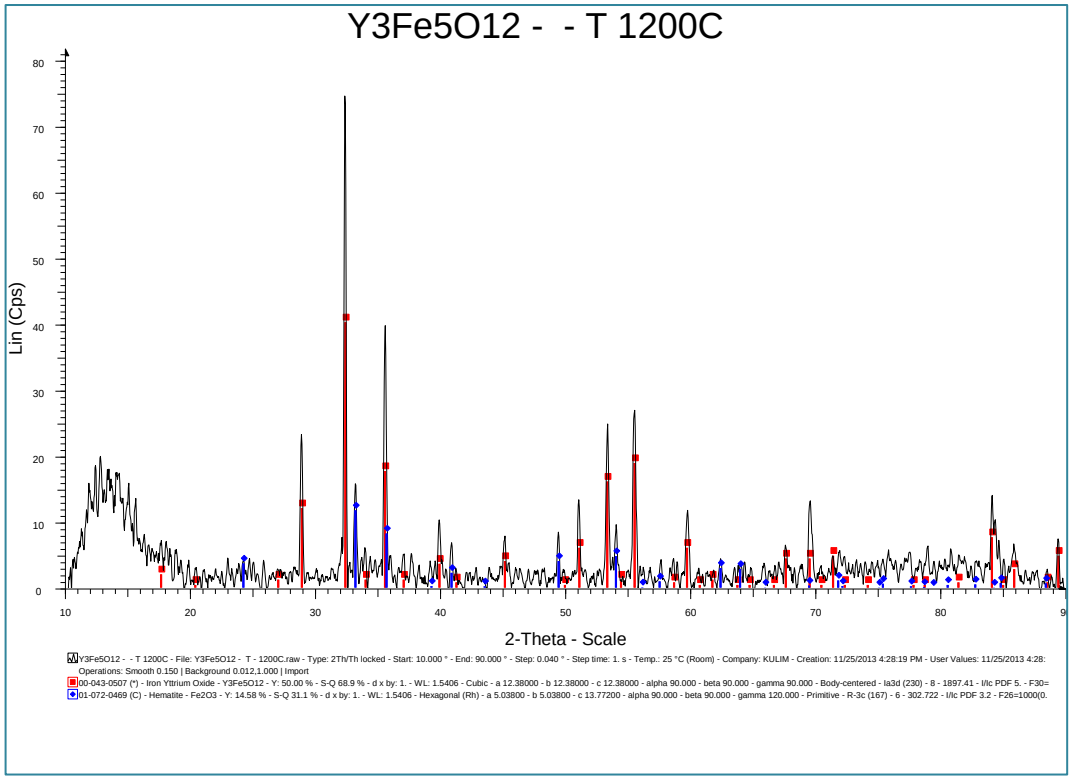

Figure 31 The XRD result of 1000°C of YIG that is re-annealed at 1200°C

Vibrating sample magnetometer (VSM) test is done to determine the magnetic properties of yttrium iron garnet (YIG) after the XRD result is confirmed that the YIG is successfully synthesize. The VSM analysis is shown in Figure 32. Briefly, looking at the graph it is shown that hysteresis loop is good in term of application of magnetic nanoparticles in enhanced oil recovery (EOR) coreflooding application with the presence of electromagnetic (EM) waves. The summary of VSM analysis of YIG at re-annealed temperature of 1000oC is shown in Table 2. From table 2, it is observed that that maximum electromagnetic unit per gram is 17.93 (emu/g) for the positive part and the maximum permeability of the sample is 0.00132 (emu/Oe).

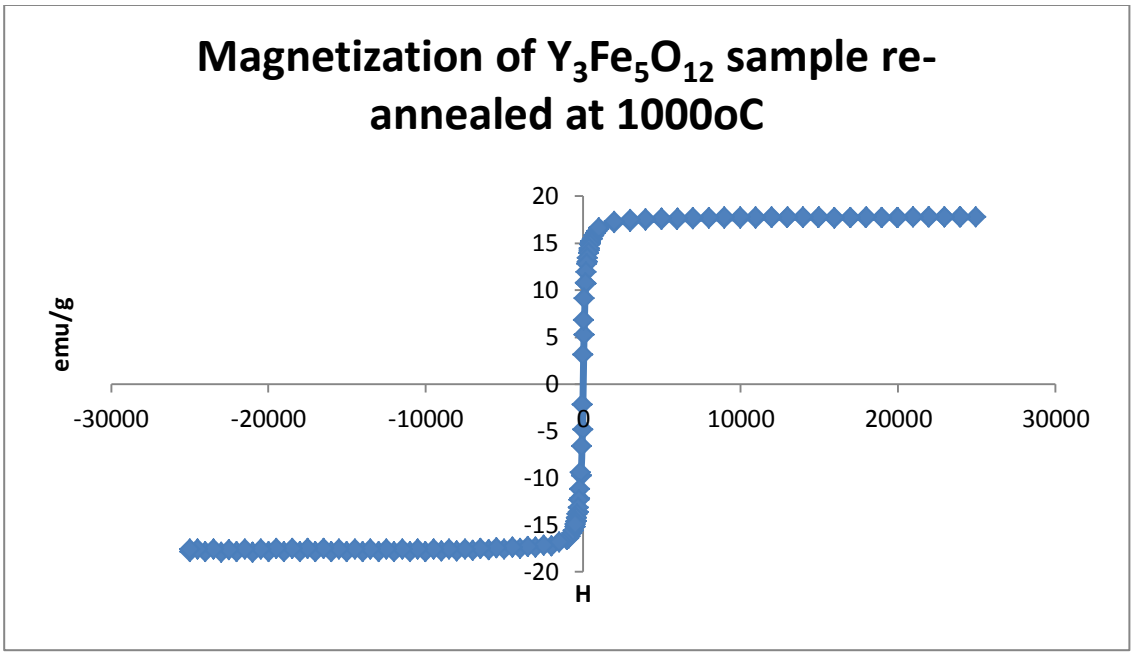

Figure 32 VSM analysis of YIG at 1000°C with citric acid as a solvent

Table 2 VSM analysis of 1000°C YIG sample

	Upward Part	Downward part	Average	Parameter 'definition'
Hysteresis Loop				Hysteresis Parameters
Hc Oe	36.080	-40.120	38.100	Coercive Field: Field at which M//H changes sign
Ms emu/g	17.930	-18.020	17.980	Saturation Magnetization: maximum M measured
Mr emu/g	-3.659	4.045	3.852	Remanent Magnetization: M at H=0
Hs Oe	1596.310	-24978.000	13287.150	Saturation field, field at which M reaches 0.95 Ms
M at H max emu/g	14.900	-14.980	14.940	M at the maximum field
Perm_90% emu/Oe	0.00003			Permeability at 90% of Ms
Perm_max emu/Oe	0.00132			Maximum permeability

The VSM result of YIG at temperature of 1200^{o}C is shown in Figure 33 and the analyzed results is shown in Table 3. Based on the result, the maximum magnetic saturation is 17.67 (emu/g) and the maximum permeability of the sample is 0.00144 (emu/Oe).

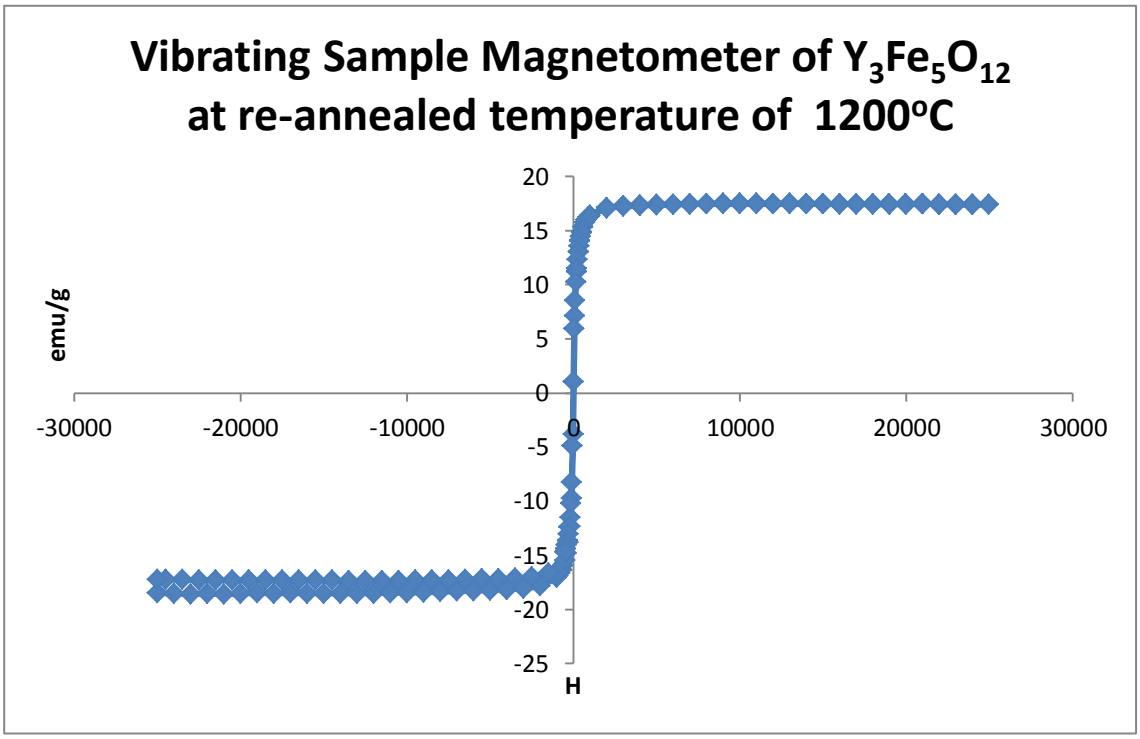

Figure 33 VSM result of $Y_3Fe_5O_{12}$ at re-annealed temperature of 1200^{o}C

Table 3 VSM analysis of YIG sample at 1200°C

Hysteresis Loop	Upward Part	Downward part	Average	Hysteresis Parameters
Hc Oe	22.90	-20.56	21.73	Coercive Field: Field at which M//H changes sign
Ms emu/g	17.67	-18.67	18.17	Saturation Magnetization: maximum M measured
Mr emu/g	-2.53	2.22	2.38	Remanent Magnetization: M at H=0
Hs Oe	1356.80	-24984.00	13170.40	Saturation field, field at which M reaches 0.95 Ms
M at H max emu/g	14.62	-15.51	15.06	M at the maximum field
Perm_90% emu/Oe	0.00004			Permeability at 90% of Ms
Perm_max emu/Oe	0.00144			Maximum permeability

Therefore, synthesizing and characterization process, yttrium iron garnet at 1200°C re-annealed temperature is chosen to be tested in the coreflooding because of the small crystallite size, high magnetic saturation in magnetic properties and high permeability counted in VSM analysis.

4.3 Coreflooding

Figure 34 shows core is setup with filling the PVC pipe with a glass beads until its fill all the space inside the plastic PVC, then 2 core holders is used to seal the glass beads. The core is sealed tightly to prevent any leaking from the core. Then, the core is weighted to obtain the dry weight. Dry weight obtained is 740.54 g.

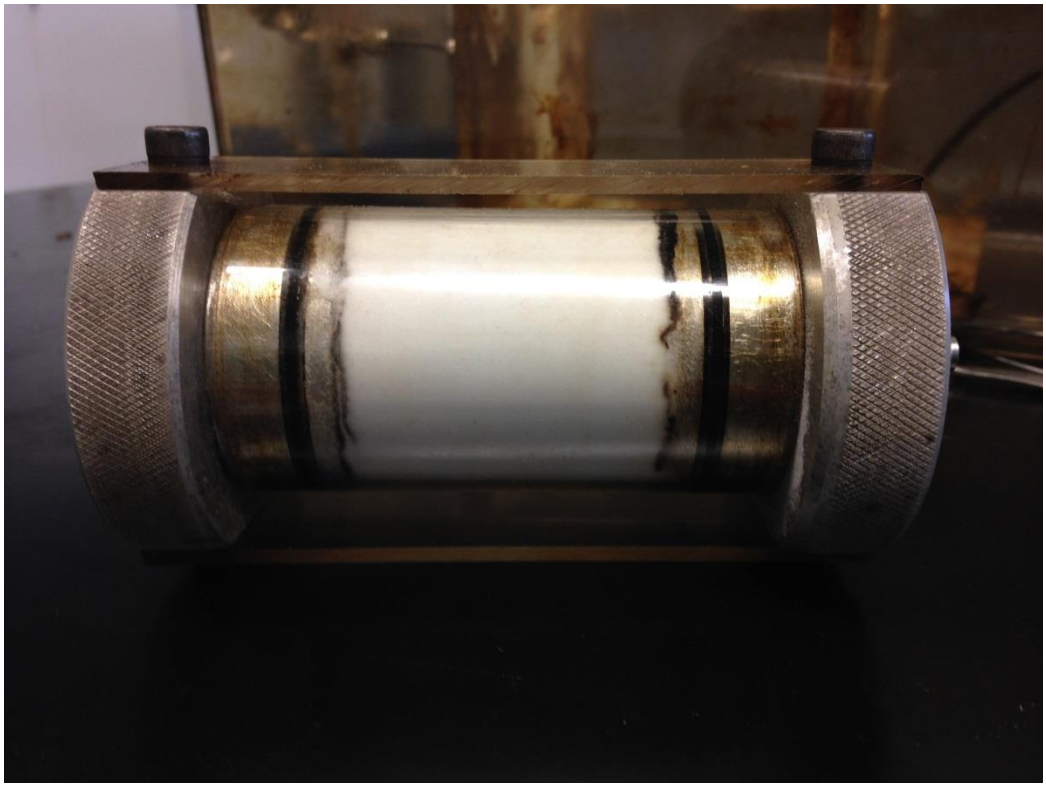

Figure 34 Core setup with a glass beads

Then, the core is saturated with 30000ppm of brine and the flowrate used in brine injection is 1 mL/min. The final volume of brine after injection is recorded at 60mL.

The wet weight of the core is 772.86g. The pore volume is calculated using the equation:

$$Pore\ Volume = \frac{(wet\ weight - dry\ weight)}{Density\ of\ brine}$$

The density of 30000ppm brine is 1.006 g/cm^3 and the pore volume calculated is 32.13 cm^3. The summarized of brine for core saturation is tabulated in Table 4.

Table 4 Core Saturation properties

Description	Value
Flowrate (mL/min)	1.00
Dry weight (g)	740.54
Wet Weight (g)	772.86
Difference in weight	32.32
Density of Brine (g/cm3)	1.006
Pore Volume (cm3)	32.13
Initial pressure (psia)	0.70
Final pressure (psia	0.30

The crude oil used in the coreflooding is heavy Iran oil. The core is saturated with the crude oil for over an hour. The volume of crude oil in the core is measured by the amount of brine that is displaced by the oil as shown in Table 5. The final volume of brine recorded is at 88mL after crude oil is injected into the core. Therefore, the volume of oil is 27mL.

Table 5 Volume of oil in the core

Description	Value
Initial volume of brine after core saturation (mL)	61
Final volume of brine after oil injected into the core	88
Volume of oil in the core (mL)	27

The secondary recovery mechanism used is waterflooding technique. The injection rate is 1.0 mL/min and the initial pressure for waterflooding is 3.0psia. The water is injected until the first water breakthrough is discovered. The volume of oil collected from water flooding is shown in Figure 35.

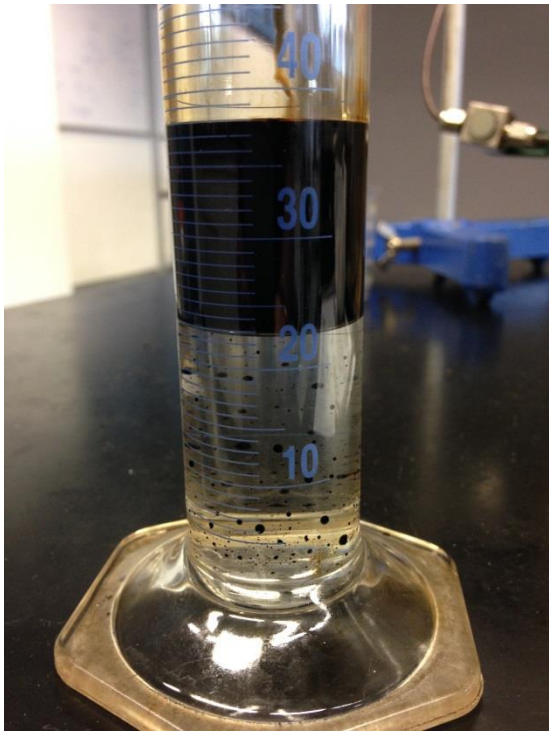

Figure 35 Volume of oil collected after waterflooding recovery technique

The summary of water injection is shown in the Table 6. The total volume of liquid collected is 38mL and the total brine collected is 22mL. The total oil recovered from the waterflooding mechanism is 16mL in which leaving 11mL of original oil in place (OOIP). The recovery factor for waterflooding mechanism is 59.26%. The core after waterflooding is shown in Figure 36.

Table 6 Oil recovery for waterflooding mechanism

Description	Value
Initial pressure (Psia)	3.00
Final Pressure (Psia)	1.30
Flowrate (mL/min)	1.00
Total volume (mL)	38.00
Volume of brine (mL)	22.00
Volume of Oil (mL)	16.00
Initial oil Volume (mL)	27.00
Remaining oil (mL)	11.00
Recovery factor (%)	59.26

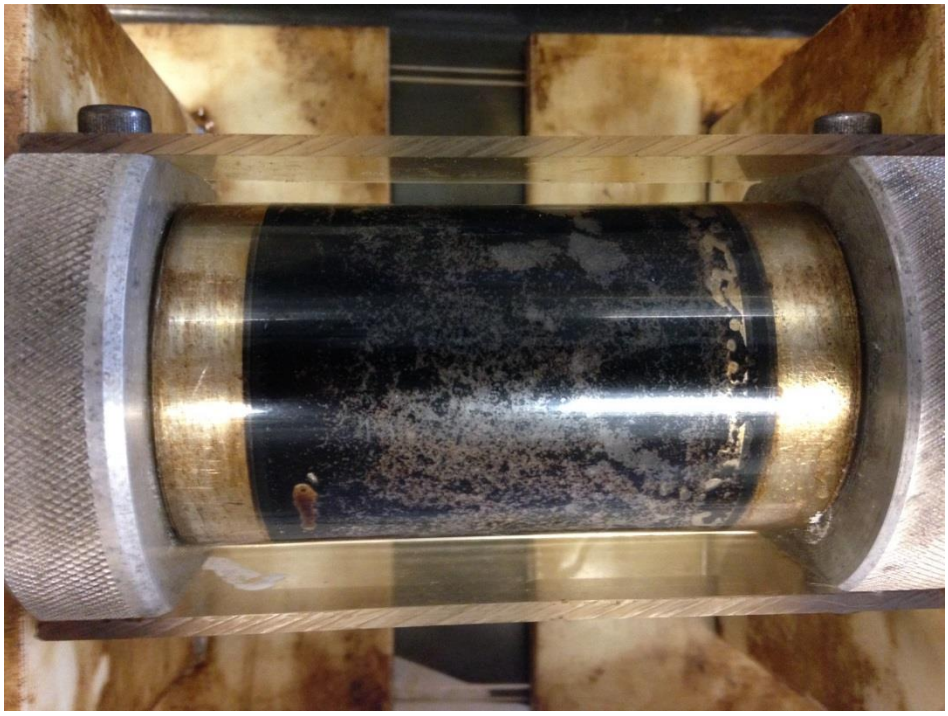

Figure 36 Condition of Core after waterflooding mechanism

The purpose of magnetic nanoparticles is to recover the remaining oil in the core. The YIG nanoparticle is prepared at 1.0wt% of 100mL. (1.0wt% = 10000mg/L = 10000ppm).1 g of Yittrium Iron Garnet (YIG) powder is diluted into 99mL of brine(30000ppm). The mixture is then slowly stirred and sonicated for 20 minutes using ultra sonic equipment as shown in Figure 37. The setup of nanoparticles injection coreflooding is shown in Figure 38. The function generator is set up at 13.6 Mhz with a square wavelength is shown in Figure 39. Water is filled up in the coreflooding tank to act as the propagating the waves.

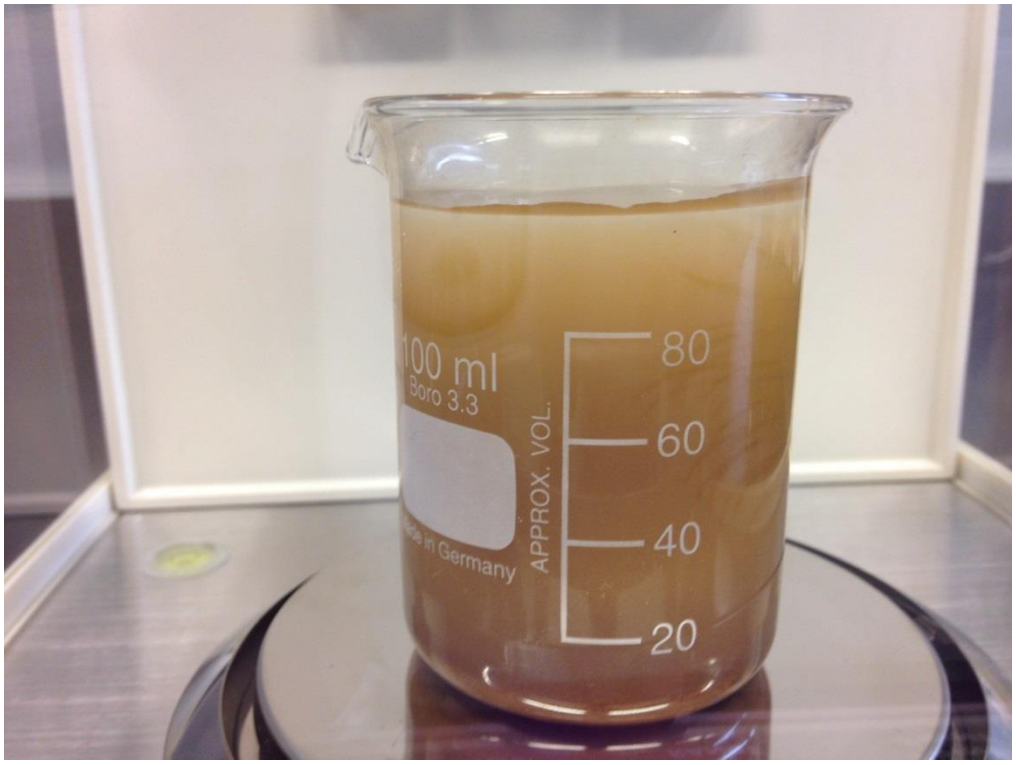

Figure 37 YIG nanoparticles after diluted with brine

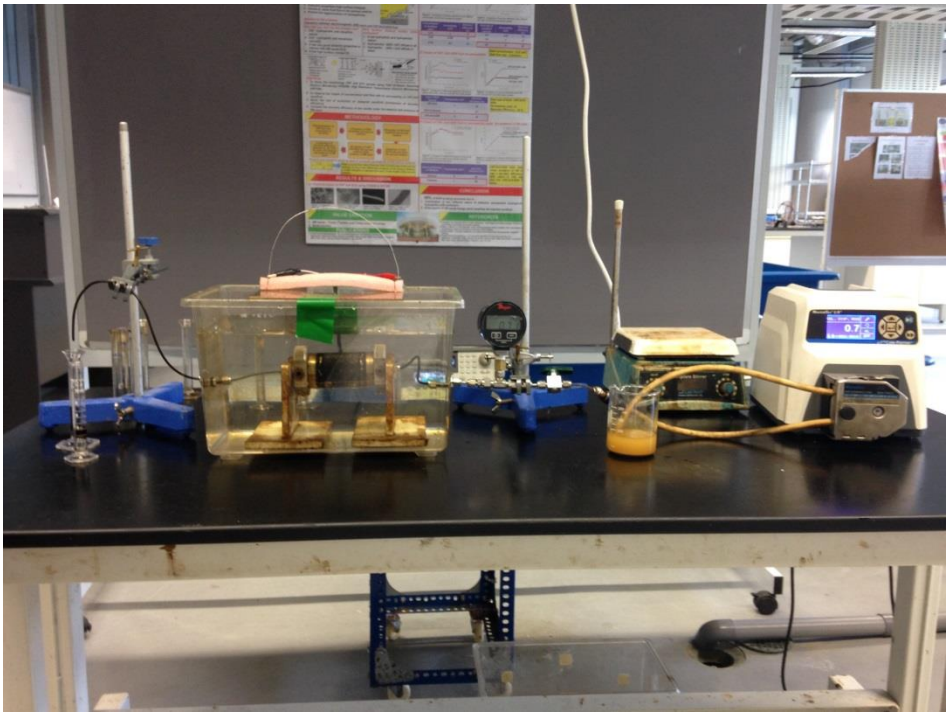

Figure 38 Coreflooding of nanoparticles with a EM waves transmitter

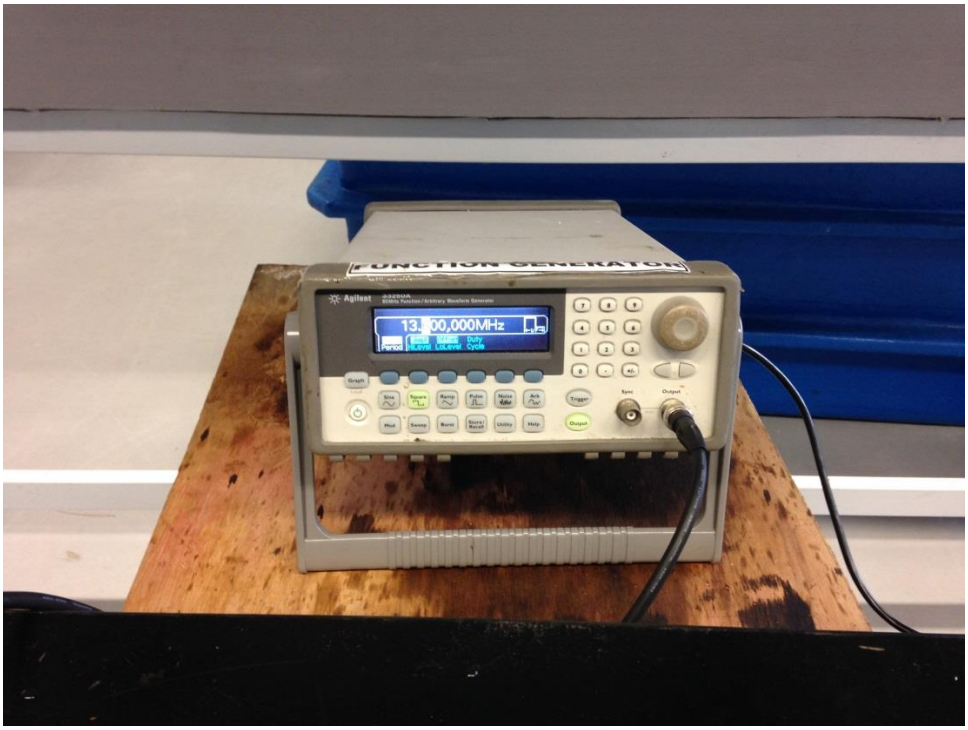

Figure 39 The function generator for the EM waves with a 13.6Mhz

A total of 2 Pore volumes (64.26mL) of YIG nanoparticles is injected in the coreflooding process. The oil is collected over 10 different pore volume. The result of the YIG coreflooding with electromagnetic waves is recorded in Table 7. A graph of pore volume with volume of oil collected is plotted to see the trends and is shown in Figure 40.

Table 7 Cumulative oil produced from the coreflooding of YIG with EM waves

Pore Volume	Initial Pressure (Psia)	Final pressure (Psia)	Total volume of liquid (mL)	Volume of brine (mL)	Volume of oil collected (mL)	Cumulative oil produced (mL)
0.2	0.77	0.40	4.20	3.80	0.40	0.40
0.4	0.70	0.60	6.80	6.20	0.60	1.00
0.6	0.66	0.35	6.80	6.20	0.60	1.60
0.8	0.62	0.13	6.80	6.20	0.60	2.20
1.0	0.56	0.24	6.40	5.80	0.60	2.80
1.2	0.50	0.18	6.50	6.00	0.50	3.30
1.4	0.48	0.37	5.40	5.10	0.30	3.60
1.6	0.43	0.13	6.40	6.00	0.40	4.00
1.8	0.37	0.24	6.40	6.00	0.40	4.40
2.0	0.30	0.18	6.60	6.20	0.40	4.80

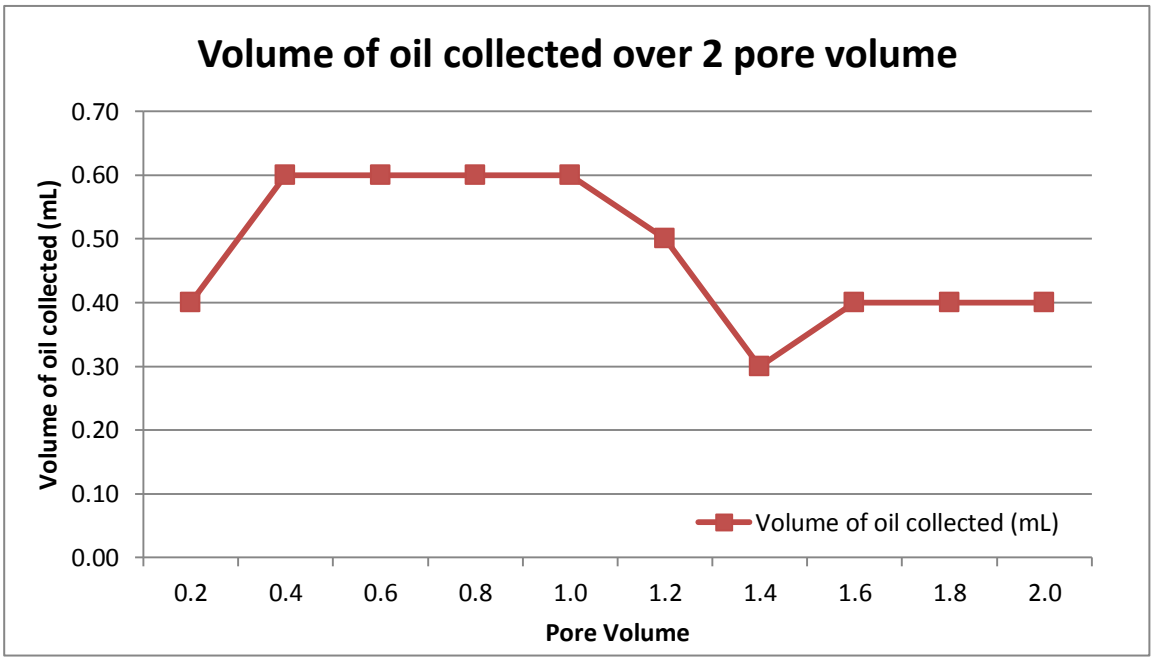

Figure 40 Oil recovery over 10 difference pore volume

The recovery factor with the pore volume is tabulated in Table 8. The highest recovery factors of the yttrium iron garnet (YIG) nanoparticles using EM waves is 2 PV in which it is able to recover 43.64% of the remaining oil in the core. The core condition after core flooding is shown in Figure 41.

Table 8 Pore volumes and recovery factors of the remaining oil in the core

Pore Volume	Cumulative oil produced (mL)	Cumulative Oil remaining in the core (mL)	Recovery Factor (%)
0.2	0.40	10.60	3.64
0.4	1.00	10.00	9.09
0.6	1.60	9.40	14.55
0.8	2.20	8.80	20.00
1.0	2.80	8.20	25.45
1.2	3.30	7.70	30.00
1.4	3.60	7.40	32.73
1.6	4.00	7.00	36.36
1.8	4.40	6.60	40.00
2.0	4.80	6.20	43.64

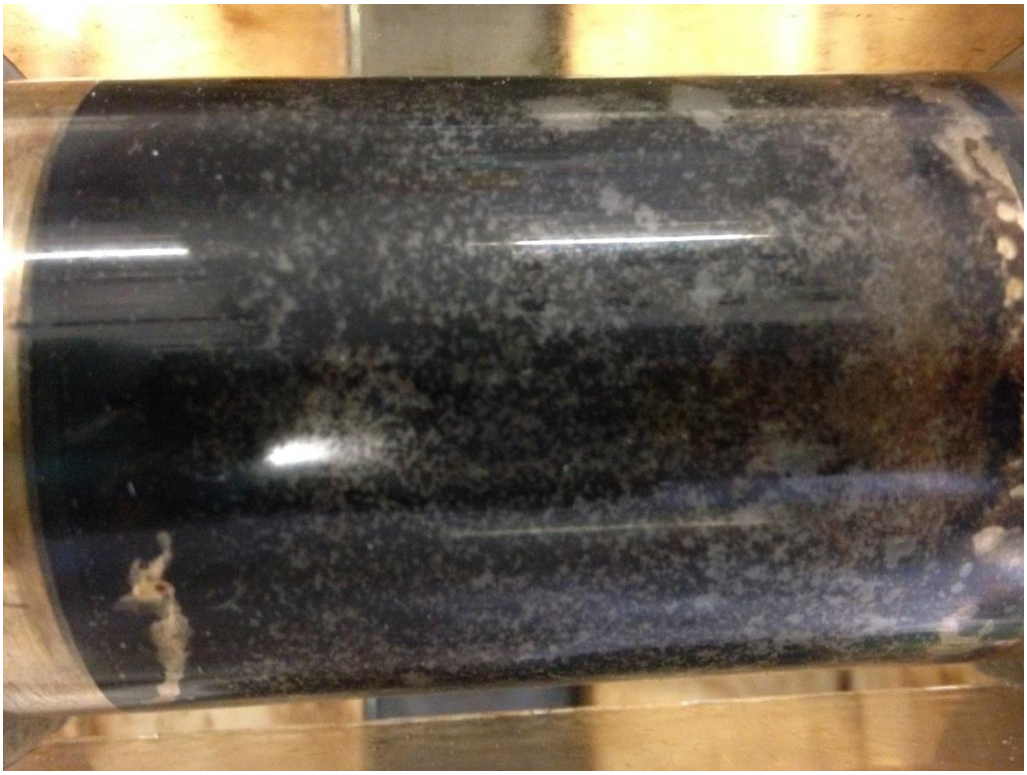

Figure 41 The core after EOR recovery mechanism through YIG nanoparticles with EM waves

The flood front of the core is analyzed to see the effectiveness of the YIG nanoparticles to sweep the remaining oil. The flood front of the core is pictured in Figure 42. Based on the Figure 42, the nanoparticles do not sweep the oil effectively because the oil portion is still remaining large at the flood front and the

Figure 42 The flood front of the core after EOR mechanism

CHAPTER 5

CONCLUSION & RECOMMENDATION

In conclusion, Yittrium Iron Garnet ($Y_3Fe_5O_{12}$) synthesized using citric acid as a solvent gives better results compare to the YIG synthesize using the nitric acid. The YIG is characterized using X-Ray diffraction (XRD), Vibrating sample magnetometer (VSM). The XRD result suggests that the sample need to go through double annealing process with an increase of temperature for the second annealing process. The results from the re-annealing process shows that the sample is successfully synthesize with a small trace of hemtatite (Fe2O3) left in the sample compared to a single annealing process. VSM analysis shows that the maximum magnetic saturation and maximum permeability of YIG is slightly higher for the higher annealing temperature. The coreflooding results shows that the recovery of YIG nanoparticles with EM waves at two pore volume yields the highest recovery of 43.64% of the remaining oil in place (ROIP). The oil recovery is 17.77% of the original oil in place (OOIP). This shows that the recovery is slightly higher compared to the literature of 10% of OOIP.

However, an improvement in the future project is required. The YIG sample is should be tested for Transmission Electron Microscopy (TEM) to determine the morphology of the sample. The YIG nanoparticles also need to be tested for the static and dynamic adsorption to determine the adsorption rate of the material. The YIG also needed to be tested for thermal stability to determine the thermal degradation of the material in order to prove the sample is able to withstand high temperature.

REFERENCES

Chiang, C.-L., Chang, R.-C., & Chiu, Y.-C. (2006). Thermal stability and degradation kinetics of novel organic/inorganic epoxy hybrid containing nitrogen/silicon/phosphorus by sol–gel method. *Science Direct*, 97-104.

China Oilfield Technology Services Group Limited. (2007). *Three Phases Of Oil Recovery*. Retrieved June 26, 2013, from China Oilfield Technology: http://www.chinaoilfieldtech.com/oilrecovery.html

Green Tech Malaysia. (2010). *National Perspective.* Retrieved February 7, 2013, from Clean Development Mechanism: http://cdm.greentechmalaysia.my/cdm-malaysia/national-perspective.aspx

Helsinki University of Technology. (2008, October 11). *Yittrium Iron Garnet*. Retrieved June 26, 2013, from Advanced Energy Systems: http://www.tkk.fi/Units/AES/projects/prlaser/YIG.htm

Islam, M., Wadadar, S., & Bansal, A. (1991). Enhanced Oil Recovery of Ugnu Tar Sands of Alaska Using Electromagnetic heating with Horizontal wells. *International Arctic Technology Conference* (p. 12). Alaska: Society of Petroleum Engineers. Inc.

Lake, D. W., & Walsh, D. P. (2008). *ENHANCED OIL RECOVERY (EOR) FIELD DATA LITERATURE SEARCH.* Austin: University of Texas.

Liu, S. (2008). *Akaline Surfactant Polymer Enhanced Oil Recovery Process.* Miami: ProQuest LLC.

Mandal, D. (n.d.). *Nanoparticles - What are Nanoparticles?* Retrieved July 6, 2013, from News Medical: http://www.news-medical.net/health/Nanoparticles-What-are-Nanoparticles.aspx

Schlumberger Limited. (2013). *Secondary Recovery*. Retrieved June 26, 2013, from Schlumberger : OilField Glossary: http://www.glossary.oilfield.slb.com/en/Terms.aspx?LookIn=term%20name&filter=secondary%20recovery

Schlumberger limited. (2013). *Primary recovery*. Retrieved June 26, 2013, from Schlumberger : oilfield glossary: http://www.glossary.oilfield.slb.com/en/Terms.aspx?LookIn=term%20name&filter=primary%20recovery

Taketomi, S., Sorensen, C. M., & Klabunde, K. J. (2000). Preparation of yttrium iron garnet nanocrystal dispersed in nanosize pore glass. *Journal of Magnetism and Magnetic Materials*, 50-64.

Tartaj, P., Morales, M. d., Veintemillas-Verdaguer, S., Gonzalez-Carreno, T., & Serna, C. J. (2003). The preparation of magnetic nanoparticles for application in biomedicine. *Journal of Physic D: Applied Physics*, 16.

United Energy Group. (2008). *Enhanced Oil Recovery.*

Vaqueiro, P., Crosnier-Lopez, M. P., & Lopez Quintela, M. A. (1996). Synthesize and characterization of yttrium iron garnet nanoparticles. *Journal of solid state chemistry*, 161-168.

Zhang, Y., & Zhai, Y. (2011). Magnetic Induction Heating of Nano-sized Ferrite Particles. In a. G. Prof. StanisA, *Advances in Induction and Microwave Heating of Mineral and Organic Materials* (pp. 485-500). Croatia: Intech.